Colección Documentos Ciemat

ANALYSIS OF CESIUM RETENTION PROCESSES IN CRYSTALLINE ROCKS

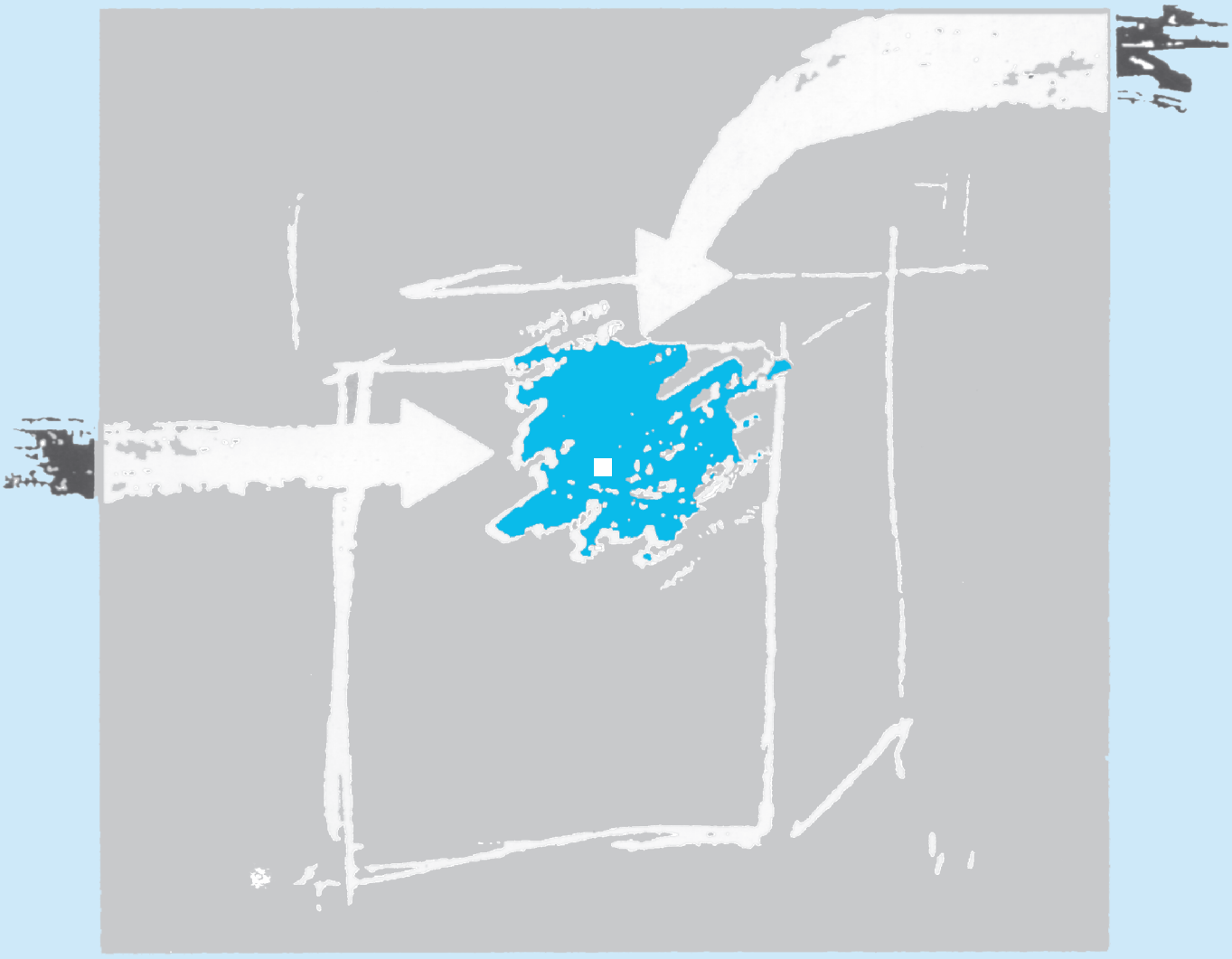

TIZIANA MISSANA
MIGUEL JULIÁN GARCÍA GUTIÉRREZ
ÚRSULA BLANCA ALONSO DE LOS RÍOS

GOBIERNO DE ESPAÑA
MINISTERIO DE CIENCIA, INNOVACIÓN Y UNIVERSIDADES
Ciemat
Centro de Investigaciones Energéticas, Medioambientales y Tecnológicas

Publicación disponible en el Catálogo general de publicaciones oficiales.

Depósito Legal: M-39691-2019
ISBN: 978-84-7834-825-1
NIPO: 693-19-045-1

Maquetación y Publicación:
Editorial CIEMAT
Avda. Complutense, 40 28040-MADRID
Correo: editorial@ciemat.es
Novedades editoriales CIEMAT

ÍNDICE

FIGURE INDEX

TABLE INDEX

1 INTRODUCTION

Deep geological repositories (DGR) are foreseen for the isolation of long-lived radionuclides. These systems are based on the multiple barriers concept, in which the barriers work together to provide redundant containment (see, for example, Chapman and McKinley, 1987; Miller et al., 2000). The main engineered barriers are metal canisters and the buffer or backfill materials, as clay and/or cement. The natural (or geological) barrier is represented by an adequate host rock formation, which must provide mechanical and chemical stability and low permeability to limit the income of water to the waste.

Favorable geological formations to host a DGR are: clays, salt formations and crystalline rocks. Crystalline rocks have been under study in different European countries as Sweden, France, Finland, Switzerland, Spain and UK (McCombie *et al.*, 1990; Riekkola *et al.*, 1999; Stanfors et al., 1999; ENRESA, 2005; Sundberg *et al.*, 2009; Chapman &Hooper, 2012) and in Canada, Japan and USA (Faurhust, 2004; Yoshida, 2005; Hansen *et al.*, 2011). The most advanced projects for DGR in Europe (Sweden and Finland) are both located in granitic formations.

Underground Research Laboratories (URLs) represented an important support to DGR - related studies; amongst those located in crystalline formations the following can be cited: the Grimsel Test Site (GTS), which is in the Aare massif of the Swiss Alps, operating since 1983; the Äspö Hard Rock Laboratory (Sweden) operating since 1995; Olkiluoto (Finland) operating since 1992; Witheshell (Canada) operating since 1984 and Mitzunami (Japan).

Sorption processes are the most important contaminant retention mechanisms and are relevant to ensure the safety of waste repositories; thus, the understanding and quantification of radionuclide sorption is fundamental for assessing the long-term behaviour of a DGR.

The performance assessment of a DGR, needs sorption data to evaluate radionuclide mobility under repository conditions. Typically, sorption is handled using the "K_d approach" and the distribution coefficients (K_d) are determined, under site-specific conditions, from static *batch* experiments with crushed rocks.

Sorption processes onto these rocks have been widely studied in the past. A critical revision of sorption data in crystalline rocks was done by Crafword *et al.* (2006) showing the problems related with the acquisition and use of K_d values in safety assessment.

The variability of K_d values obtained (supposedly) in similar experimental conditions typically may span over 2-4 orders of magnitude, even when the same material is considered. This sorption variability seems not to be representative of true mineralogical or aqueous geochemical variability, therefore the sources of these uncertainties must be pointed out, to overcome the lack of the mechanistic description of the retention processes in these systems. Payne *et al.* (2013) evidenced that, in the context of radioactive waste disposals, the K_d approach has many drawbacks, and that a more mechanistic approach to retention processes is needed, to estimate their uncertainties in a sound way and to support a defendable choice of K_d values. Nowadays, mechanistic models are sometimes used to provide support to expert judgment for K_d selection for PA models, but their

application is very limited, above all in crystalline rocks, because a convincing picture of how retention processes should be modelled in these systems is still lacking; additionally, it is indeed complicated to apply a mechanistic model when uncertainties on the reliability of experimental data still exist.

The objective of this document is to analyse Cs sorption data obtained in different crystalline rocks and comparing them to evaluate the possible causes of their spreading for building the basis for the application of predictive sorption models.

^{137}Cs (half-life, ~30 years) is an important fission product from the irradiation of uranium-based fuels and its inventory in nuclear waste is high. It is a radionuclide of special environmental interest as, in the past, it has been released to soils and waters upon nuclear accidents or weapon testing (Steinhouser, 2014). Tt exists predominantly as the monovalent cation Cs^+, which present very high solubility; furthermore, for its simple chemistry, it has been considered an adequate radionuclide for carrying out this study.

Crystalline rocks are characterized by mineralogical heterogeneity and retention processes may comprise ionic exchange (with constant-charge minerals like micas and clay minerals) and/or surface complexation (with minerals exhibiting pH-dependent surface charge). However, cesium adsorbs onto natural solids mostly by ionic exchange (Missana *et al.*, 2014) thus the extent of its uptake depends on the properties of the solids i.e. their cation exchange capacity (CEC), but also on the presence of *mica-like* minerals, which present sorption sites with high selectivity for alkali cations (Sawhney, 1970, 1972; Poinssot *et al.*, 1999; Zachara *et al.*, 2002).

In this work, to limit the experimental uncertainties all the experiments were carried out with different crystalline rocks but under as similar as possible chemical conditions. The effects of several parameters as time, Cs concentration, pH and water salinity on K_d values were investigated. Data were also analyzed with the aim of evidencing the possible differences in the sorption behavior, caused by the different rocks' properties (minerals content, BET area) and considering the existence of competitive ions in solution. The new experimental data were compared with older data obtained at CIEMAT, when available.

In all the granites studied, Cs sorption showed a non-linear behaviour, a small dependence on the pH and significant dependence on the ionic strength. This indicates that the main retention mechanism is ionic exchange, controlled by the presence of more than one adsorption site. The presence of potassium as competitive ion is very important in the overall Cs retention, especially when Cs is present at low concentrations.

The final aim of this work is providing inputs for a mechanistic treatment of sorption data and for the application of thermodynamic models, which requires more detailed information. The evaluation of the data presented in this document, includes a simple modelling based on a *top-down approach*, which main objective is to reproduce correctly the main source of variability in the distribution coefficients of cesium, pointed out by the experimental data, and especially: Cs concentration, ionic strenght and pH of the water and the presence of potassium as main competing cation.

2 CRYSTALLINE ROCKS

Crystalline rocks (saturated and sparsely fractured rocks) are generally composed of a variety of different minerals (mainly quartz, feldspars, micas and other accessory minerals) with typical sizes of the order of millimeters to centimeters. Minerals as quartz, albite (plagioclase), muscovite, biotite, chlorite, olivine, epidote, and hornblende are usually present in these materials. The mineral grains, with both inter-granular and intra-granular porosity, constitute the so called "*rock matrix*". The *porosity* of the intact rock matrix is small, typically few tenth of a percent; altered rocks may present porosity up to one order of magnitude higher.

Crystalline rocks are heterogeneous systems on different scales. The smallest heterogeneities, relevant for solute transport or sorption, are in the μm-cm scale, due for example to mineral grains and pore distribution. Heterogeneities at much larger scales (m-km) are also of importance for water flow and transport. Due to the physical and chemical heterogeneities, the description of the water flow paths and solute transport in of crystalline media is an issue for the performance assessment of waste repositories.

Radionuclide sorption is expected to occur at the surface of the fresh material, but due to the weathering and alteration of the major rock components, water conductive fractures may contain fillings of different minerals. The nature of these fracture fillings depends in a large extent to the nature of the primary rock, but minerals commonly found are: quartz, secondary mica minerals, iron oxy-hydroxides, oxides, calcite and other carbonates and clay minerals.

They further diversify the physical - chemical properties of the transport paths. Furthermore, they have higher porosity, surface area and CEC than the bulk rock. Thus, fillings usually present higher sorption capacity and may present an important role in radionuclide retardation. Nonetheless, at a larger spatial and temporal scale, sorption into fillings might be of secondary importance, as the mass of the "rock matrix" is predominant, for this reason they are not considered in performance assessment.

In this study, different types of crystalline rocks were used, and their characteristics will be summarized in the next paragraphs. These solids are original from different countries (Switzerland, Spain, Sweden) and have been obtained and characterized during CIEMAT`s participation in national and international projects on radioactive waste management over the years. The basic information will be given in the text and more details on the materials will be provided in the Annex to this document.

2.1 CRYSTALLINE ROCKS FROM SWITZERLAND

The rocks come from the Grimsel Test Site (GTS), which is an underground laboratory where many experiments, devoted to analyze the behavior of a DGR in a granitic formation, at 400 mt in depth, and radionuclide migration in fractured rocks, have been carried out for more than 25 years in different existent experimental tunnels (Hadermann & Heer, 1993).

In the northern part of the GTS, the granite is of *Central Aare type* and in the southern part granite is of granodiorite type (Schneeberger et al., 2017).

2.1.1 GRANITE FROM THE FEBEX TUNNEL AT GTS (G-FEB).

The FEBEX tunnel has been the site of different experimental tests at the GTS, within several international projects as FEBEX, FEBEX II or FUNMIG. The granite coming from this area corresponds to the to the central Aare type. The rock used for sorption experiments was taken from a cylindrical block (sample RB0-1) obtained at site (Figure 1, left). This block was used to carry out a medium scale diffusion experiment (see Figure 1, right), with Cs, Cl and tritiated water, HTO, which is still running at CIEMAT (Samper *et al.*, 2009).

The samples from sorption experiments with granite from the FEBEX tunnel (*G-FEB*) were taken from the central part of this block. The material was crushed and sieved to obtain three different fractions (F1, F2 and F3).

The mean mineralogical composition of this granite is given in the Annex (Table_A1).

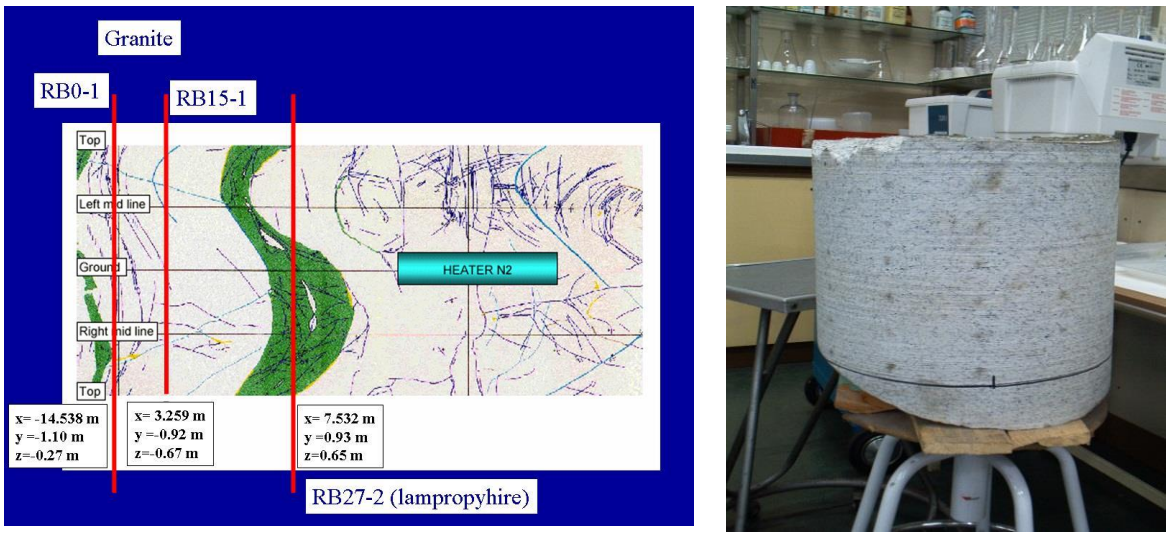

Figure 1. Schematic of the FEBEX gallery with the indication of the location where the RB0-1 block (right) was drilled. The material used for sorption tests was obtained from the central part of this block.

2.1.2 GRANITE FROM THE MIGRATION TUNNEL AT GTS (G-MIG).

The material used for sorption experiments comes from the shear zone that was selected for the CRR (Colloids and Radionuclide Retardation) experiment (Mori *et al.*, 2003), located at the Migration tunnel (BOEX 97.001). The characteristics of this *granodiorite* and of fracture filling materials of this zone are largely described in the literature and they are summarized in Table_A1. With respect to the granodiorite, the fracture material (defined as mylonite or proto-mylonite) is characterized by higher sheet silicate content and by higher muscovite content. Mylonite also presents a lower FeO content (1.1 - 1.5 wt%) than the granodiorite (3.3 wt%), which indicates that the quantity of Fe(II)-bearing minerals is higher in granite than in the fracture material (Missana & Geckeis, 2006).

In the core material used for the experiments, two different regions were distinguished at sight: one of them, darker, probably due to its higher biotite content, which was denominated as *"black"* granite. The sorption behavior of both black (*bG-Mig*) and standard *G-Mig* was analyzed for comparison. In Missana & Geckeis (2006) it was observed that the iron content was significantly higher in the "black" granite than in the normal one.

2.2 CRYSTALLINE ROCKS FROM SPAIN

Two different Spanish crystalline rocks were analyzed. The first one comes from *Los Ratones* mine (Gomez, 2002; Marcuello et al., 2006) and the second one from the *El Berrocal* site (Rivas et al., 1997). Both granites were previously studied at CIEMAT in the frame of the ENRESA-CIEMAT association in various projects.

2.2.1 GRANITE FROM "LOS RATONES" MINE (RAT).

Los Ratones mine was in the Albalá (Cáceres) granitic pluton. Five boreholes were drilled in the mine zone to make a detailed hydrogeological study. A thorough characterization of the sorption properties of materials extracted from different boreholes in *Los Ratones* mine were carried out, as well as of their chemical characterization. More details on the characteristics of this granite can be found in (Gomez, 2002).

At the *Los Ratones* site four types of granite facies were distinguished: they were named *Millares*, *Perdices*, *Cabeza Porquera* and granite with large crystals, *Megacristales*). The mean mineralogical composition of these different types is summarized in the Annex (Table_A2).

The characteristics of the granite, as well as its degree of alteration, varied from a borehole to another and with the extraction depth (Table_A3). The reference granite, representative of fresh granite, was of *Perdices* type, extracted from the borehole 5 (SR-5) at a depth of 321-324 mt. The sorption in the rocks from all the existing boreholes SR-1, SR-2, SR-3, SR-4 and SR-5 was analyzed in previous studies (García-Gutiérrez et al., 2000).

2.2.2 GRANITE FROM "EL BERROCAL" (BER)

The *El Berrocal* site was located 90 Km southwest Madrid in the central part of the Centro-Iberian Zone. The site belongs to a granite pluton, hosting uranium mineralization mined until late sixties. A detailed description of the site and the experimental activity carried out in there can be found in Rivas et al. (1997). The *El Berrocal* granite was formed by three different granite facies (*El Berrocal* facies (the main one), *El Berrocal* leucogranites, *El Berrocal* pegmoaplites. The granite considered as the reference (fresh) material was that from the borehole named S-16. This reference granite is holocrystalline, medium-grained size and can be defined as two micas, alkali feldspar quartz granite with dominant muscovite and biotite as the scarcest mineral. Amongst the alteration processes observed, it can be mentioned the chloritization and moscovitisation of the biotite, the sericization of the plagioclase and interstitial albitization, that give rise to an increase of granite permeability. The material coming from the S-15 borehole, represents the weathered granite. The main mineralogical characteristics of the reference *(Ber)* and weathered *(w-Ber) El Berrocal* granite are summarized in the Annex (Table_A4).

Several authors state that is of great interest to analyze more in detail the retention properties of the altered rock, because it provides larger pore volume for radionuclides to migrate and higher surface area for sorption processes (Yoshida et al., 2009). This statement appears true in several cases, however, the influence of alteration and weathering on sorption properties has been reported to depend on the rock type. Cui and Eriksen (1996) suggested that granite fracture filling material had a lower sorption capacity for Cs than fresh Stripa granite; less Cs sorption was also observed in Äspo weathered granite, whether other authors do not observe big differences from fresh to altered granite (Kienzler et al., 2004)

Previous studies on the El-Berrocal granite were carried out at CIEMAT by García-Gutiérrez (1994).

2.3 CRYSTALLINE ROCKS FROM SWEDEN

2.3.1 GRANITE FROM THE ÄSPÖ HARD ROCK LABORATORY (ÄS)

The Äspö hard rock laboratory (Äspö HRL), is a research facility where much of the research about the Swedish final repository for spent nuclear fuel is taking place. Äspö HRL is in the Simpevarp area in the municipality of Oskarshamn. The Äspö island is located 30 km north of the center of Oskarshamn and close to the nuclear power plants. The underground part of the laboratory consists of a main access tunnel from the Simpevarp peninsula to the southern part of the island Äspö where the tunnel continues in a spiral down to a depth of 460 m. The depth of Äspö HRL is 0-460 m.

The two dominant crystalline rock types at the site are the Äspö diorite (quartz monzodiorite to granodiorite, porphyritic) and Äspö granodiorite (granite to quartz monzodiorite, generally porphyritic). The rock used for the experiments (diorite) was provided in two different fractions (fine and gross) (*Äs-f* and *Äs-g*, respectively). More information on this rock can be found in Johnsson et al. (1998).

3 MATERIALS AND METHODS

3.1 SUMMARY OF THE SOLIDS USED FOR SORPTION TESTS

For the sorption experiments reported here, crystalline rocks from the different sites described in the previous paragraphs were used. Two granites come from the GTS (Switzerland): one from the FEBEX tunnel, from here to hereafter referred to as Grimsel FEBEX granite (*G-FEB*) which corresponds to the central Aare type, that was used in three different fractions (*F1, F2* and *F3*).

The second type of granite comes from the Migration tunnel, it corresponds to a granodiorite type, which will be referred to hereafter to as Grimsel Migration granite (*G-Mig*). In this material the darker (black) part was isolated and crushed separately from the rest and it will be defined as (b*G-Mig*).

Three granites come from Spain: the first one from *Los Ratones* mine, *Rat* granite, and two different from the *El Berrocal* site (a fresh one, *Ber*, and a weathered one, *w-Ber).* The last rock comes from the Äspö Hard Rock Laboratory (Sweden), which has been used in two different fractions: fine and gross, called *Äs-F* and *Äs-G*, respectively.

COUNTRY	SWITZERLAND		SPAIN		SWEDEN
MINERAL (%)	G-Feb	G-Mig	Rat	Ber	Äs
Quartz	30-36	25-31	33-35	**40-43**	14
Plagioclase /Albite	19-23	26-32	29-32	28-31	**45**
K-Feldspar	31-37	22-26	26-28	**15-18**	15
Biotite /Chlorite	6-8	**10-12**	2-3	2-3	**15**
Muscovite	1-2	3-4	5-6	**7-9**	--

Table 1. Main mineralogical composition of the granites used in the experiments.

Table 1 shows the main mineralogical composition of the different (fresh) granites. The principal composing minerals in crystalline rocks are quartz, plagioclase/albite, K-feldspar, biotite and muscovite. The highest quantity of quartz is present in the *El Berrocal* granite, whether the *Äspö* diorite has a significantly lower quartz than any other granite. Instead, *Äspö* rock has the highest quantity of plagioclase and biotite. The lowest quantity of biotite is clearly present in the granites from Spain.

It is expected that the different mineralogical composition may affect radionuclide retention in the different crystalline rocks; to prove that, additive models may be used to explain the overall sorption in these complex materials. To do that, a detailed sorption study on several composing minerals has been done which results will be summarised elsewhere.

Table 2 shows the summary of all the crystalline rocks used for sorption experiments, indicating their size fraction and their BET surface area. The *G-FEB* and the *ÄsF* granites showed very small surface area (<0.1 m^2/g) in all the fractions considered, whereas in *G-Mig* and *Ber* rocks the BET

area was up to an order of magnitude higher. The *Rat* granite has an intermediate BET area and, finally, the weathered material from *El Berrocal, w-Ber*, presented the highest BET, in agreement with its degraded state.

SAMPLE	SIZE FRACTION x (mm)	BET (m^2/g)
G-Feb (F1)	x < 0.5	0.09±0.02
G-Feb (F2)	0.5< x <2	0.08±0.02
G-Feb (F3)	2< x <4	0.03±0.01
G-Feb(F2), washed	0.5< x <2	0.04±0.02
G-Feb(F3), washed	2< x <4	0.01±0.01
bG-Mig	x<0.064	4.10 ±0.01
G-Mig	x<0.064	2.87±0.01
RAT	x< 1	0.49±0.01
Ber	x<0.5	2.78±0.01
w-Ber	x <0.064	40.20 ±0.01
Äs-F	1<x<2	0.09±0.02
Äs-G	2<x<4	0.07±0.02

Table 2. Size fraction and BET areas of the rocks used in sorption experiments.

In Table 2 two additional samples are mentioned: "washed" *G-Feb (F2)* and *G-Feb* (*F3).* This is because after the first experiments, it was noticed these larger fractions, had some fine particles attached and therefore they needed a careful washing. The BET after washing was measured and confirmed the probable bias of the first results obtained by this fine material. Thus, the larger fractions were always washed from fine ones before their use. In summary, the selection of materials covers a wide range of characteristics (BET, size fraction and mineralogy), data that can be related to the overall sorption properties of the different solids.

3.2 AQUEOUS SOLUTIONS

A "typical crystalline" groundwater cannot be defined. Water composition can be very different from a formation to another but, in general, redox conditions at repository depth are expected to be reducing. Table_A5 to Table_A7 in the Annex show examples of the composition of different waters from the granitic rocks considered in this study. In general, groundwaters from the GTS in Switzerland are low saline ($I \sim 10^{-3}$ M) and alkaline (pH 8-10) as shown in Table_A5, where the chemical composition of waters sampled from both the *Migration* and *Febex* tunnels is detailed.

The groundwaters from the Spanish sites (*Los Ratones* y *El Berrocal*) are relatively low saline waters but their electrical conductivity is slightly higher that of GTS' waters, as can be seen in Table_A6. In this Table, the composition of a Spanish commercial granitic water used in the past for sorption experiments is also included.

Finally, the groundwater from the Äspö Hard Rock Laboratory, can be affected to a different extent by the presence of the sea, and presents much higher ionic strength than the others. Table_A7 shows the composition of the water sampled near the zone in which the solids used for sorption experiments were obtained.

ELEMENT (mg/L)	LSW	HSW	SYNTHETIC ÄSPö
Na^+	8.3	1,8	1,7
Ca^{2+}	7	1,000	1,200
Mg^{2+}	<0.03	0.09	105
K^+	<0.03	<0.1	0.42
Cl^-	28	4600	13
SO_4^{2-}	<0.1	0.42	4,700
F^-	<0.1	<0.1	400
Al	<0.03	<0.03	17
Fe	<0.03	<0.03	1.2
Cs	<0.02	<0.02	< 0.03
Si	0.69	<0.3	< 0.03
Alk (meq/L)	<0.05	<0.1	< 0.03

Table 3. Chemical composition of the aqueous solutions used in the experiments

To perform sorption studies, different simplified aqueous solutions, representing different possible granitic waters were produced: a *low* and a *high* saline water (LSW and HSW respectively) and a water representative of the Äspö groundwater, based on the analysis of natural water reported in Table_A7, with a simplified composition. This water was called Synthetic Äspö water. In respect to the HSW, it presents high sulphate content, which could be a significant element in the case of anion sorption. The main composition of the three waters used in sorption experiments is summarized in Table 3. To prepare the synthetic waters, all the reagents were of analytical grade and they were used without further purification.

In order to evaluate the possible leaching of ions upon water-rock interactions the composition of waters after 1 month of contact with the solids was analyzed (except in the case of *G-FEB* granite where it was followed for approximately half an year), as will be detailed in later in the results section.

3.3 RADIONUCLIDE

The radionuclide used in this study was ^{137}Cs (as CsCl in 0.1 HCl). The half-life of ^{137}Cs is 30.2 years. The activity of cesium in solution was measured by γ-counting with a NaI detector (Packard Autogamma COBRA 2).

3.4 BATCH SORPTION TESTS

Sorption experiments with the Äspö diorite were carried out in a glove box under N_2+CO_2 atmosphere, to preserve the characteristics of the recently drilled samples, whereas the tests with the

other solids, were carried out under aerobic conditions. Cesium is not a redox sensitive element, and therefore no large differences are expected in its sorption under anoxic or aerobic conditions. All the tests were done at room temperature (22 ± 2 ºC).

In the experiments, a similar experimental systematic was followed for all the rocks. *Kinetic* experiments were carried out with cesium concentrations of approximately $5 \cdot 10^{-9}$ M and pH approximately 7; the dependence on pH was evaluated, carrying out sorption edges changing the pH from approximately pH 6 to 10 and with the same Cs concentration as that used in kinetic experiments. No pH buffers were used to stabilize the pH.

Sorption isotherms were carried out at pH 7.0±0.5 covering a concentration range of more than six orders of magnitude (10^{-9} to 10^{-2} M). If previous data obtained for Cs sorption on the same materials were available, they were compared with the new ones. Preliminary kinetic tests were useful to determine the contact time needed to reach the sorption equilibrium. In general, Cs sorption kinetics was negligible for the finest sample used (<0.5 mm) whereas (progressively) increased for the largest ones. The rest of experiments, if not specifically indicated, were carried out with a contact time of 14 days.

To perform batch tests, ten mL of the initial aqueous solution were introduced in polyethylene centrifuge tubes where the solid was added. Before the addition of the radionuclide, the solid and the water were equilibrated at least 1 day. Samples were prepared in duplicate for finest fractions and in triplicate for the largest fractions, because the heterogeneity of the samples may be higher. Three aliquots for each sample (2 mL) were taken for the measurement of Cs activity. After the water/solid equilibration, the radionuclide was added, and the pH adjusted if necessary. The tubes with the solid and the liquid were maintained under continuous stirring during the selected contact time. They were later centrifuged (26000 g, 30 min). After the solid separation, three aliquots of the supernatant from each tube were extracted for the analysis of Cs final activity. The rest of the solution was used to check the final pH.

The distribution coefficients were calculated using the formula:

$$K_d = \frac{Cs_{ADS}}{Cs_{FIN}} \cdot \frac{V}{m} \qquad \text{Equation 1}$$

where Cs_{FIN} the final concentration of cesium in the liquid phase, Cs_{ADS} is the adsorbed cesium (Cs_{INI} - Cs_{FIN}), *V* the volume of the water and *m* the mass of the solid.

All the data presenting an error *higher than 5 % in the activity measurement* were discarded considering that this deviation can only be related to experimental problems (e.g. inaccurate centrifugation or phase separation). Nevertheless, the difference on sorption coefficients measured in different samples of the same rock, represents the real heterogeneity of the material, especially when large size fractions are used, and it must be accounted for.

3.5 MODELLING OF EXPERIMENTAL DATA

In this study, the main objective of the modelling was trying to elucidate the principal causes of K_d values spreading, when considering different crystalline rocks. For this reason, the modelling was based in a simple top-down approach, based in the overall mean properties of the materials. The differences of Cs sorption from a material to another will be pointed out as well as the needs for a more precise and mechanistic modelling.

Cesium sorption onto minerals, and especially on micas, is expected to occur by ionic exchange reactions. The ionic exchange reaction between a cation B, with valence z_B, present in the solution and the cation A, with valence z_A, on the solid surface (≡S) is defined by:

$$z_B A \equiv S + z_A B \Leftrightarrow z_A B \equiv S + z_B A \qquad \text{Equation 2}$$

Using the mass law equation, it is possible to express the ion Exchange relation in terms of selectivity coefficient, K_{SEL}. According to Gaines and Thomas (1953), the selectivity coefficient between cations A and B is defined as:

$$^{B}_{A}K_{SEL} = \frac{(N_B)^{Z_A}}{(N_A)^{Z_B}} \cdot \frac{(a_A)^{Z_B}}{(a_B)^{Z_A}} \qquad \text{Equation 3}$$

where a_A y a_B are the activities of cations A and B, and N_A and N_B the fractions sites in the solid occupied by A and B, respectively.

For sake of simplicity, all the rocks were assimilated to simple monovalent exchangers, being the main reaction:

$$M \equiv S + Cs \Leftrightarrow Cs \equiv S + M^{+} \qquad \text{Equation 4}$$

Depending on the shape of the experimental sorption isotherms, one or more sorption sites will be used to perform data fit.

If in some case, Cs sorption would show a non-negligible dependence on pH, surface complexation reactions will be considered. In this case, considering amphoteric surface functional groups at the rock surface, SOH, reactions of this type must be accounted for:

$$SOH + Cs \Leftrightarrow SO - Cs + H^{+} \qquad \text{Equation 5}$$

The modelling calculations were done with the CHESS v 2.4 code (van der Lee & De Windt, 1999), and the fits of the experimental curves were obtained with a trial and error procedure.

4 RESULTS AND DISCUSSION

4.1 WATER SOLID INTERACTIONS

The kinetic of water-solid interactions was analysed to determine the type and extent of ions leached from each solid in contact with the aqueous solutions. Even if the initial electrolyte is initially the same, each mineral or rock interacts with the liquid phase; due to dissolution, ion exchange or other process, the composition of the water at the equilibrium can be different. The analysis of these possible differences is fundamental to clarify phenomena of ion competence or any other deviations from the expected sorption behaviour.

Competitive cations present in solution may play a significant role in Cs retention and they may be an important source of variation in the value of distribution coefficients. The determination of selectivity coefficients can be biased if the presence of competing ions is not accounted for (Missana et al., 2014).

The solids were dispersed in the low saline water, LSW, because the differences are expected to be more evident. The experiment lasted approximately one month for all the solids, but in the case of *G-FEB* granite, the contact time was increased up to approximately half a year. The results of the test for the three fractions of the *G-FEB* is summarized in Table_A8 of the Annex. The solid to liquid ratio was that used for sorption tests (10 g/L).

Results showed that a no negligible increase of conductivity is present since the very beginning of the experiment, indicating the dissolution of some soluble trace mineral (Table_A8). The increase in Ca^{2+}, K^{+}, F^{-}, Cl^{-} and SO_4^{2-} and alkalinity is observed, with stable values maintained after the initial rapid increase.

Of possible interest in the case of cesium sorption is the increase in K^{+}, which will be accounted for in the interpretation of data. No large differences were observed using different size fractions of the granite and at very large contact times. Table 4 shows the values of potassium measured in all the analyzed waters after 1 month of contact with the solid phase. Non negligible quantities of potassium are always released from the solid phases; this experimental "problem" can be more evident using higher solid to liquid ratio and this must be accounted for in the overall evaluation.

SOLID	K+ (mol/L)
G-Feb (F1)	8.5E-05
b-GMig	2.6E-04
G-Mig	2.5E-04
Rat	5.4E-05
Ber	5.1E-04
w-Ber	1.0E-04
Äs-f	6.9E-04
Äs-g	5.4E-04

Table 4. Potassium content in the LSW after 1 month contact with the solids (10 g/L)

4.2 SURFACE CHARGE

Before starting sorption experiments the surface potential (zeta-potential) of four rocks as a function of the pH was measured by laser Doppler electrophoresis with a Malvern Zetamaster apparatus. The surface charge is one of the important parameters driving sorption processes because the surface-ion attraction is the first step to ion retention.

The results obtained for zetapotential measurements are shown in Figure 2. The surface charge of all the rocks is always negative and constant between -50 and -60 mV for neutral and basic pH.

It is interesting observing that, despite their mineralogical differences, observed in Table 1, the overall charge behaviour of the analysed rocks is quite similar.

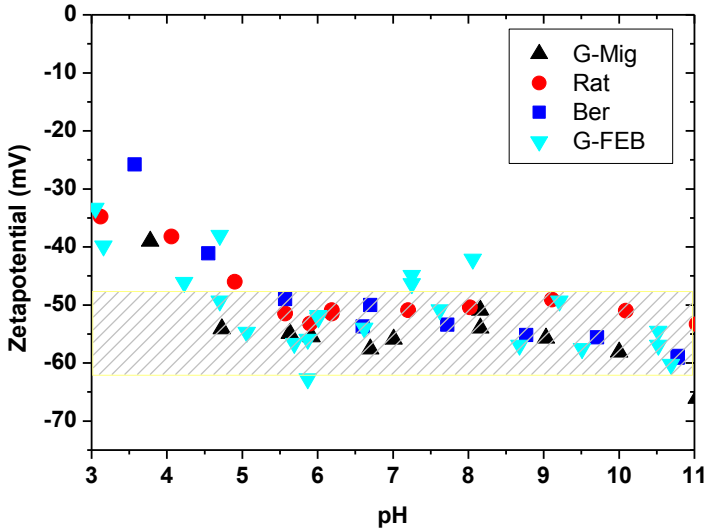

Figure 2. Zetapotential of different granites as a function of the pH.

4.3 SORPTION TESTS

4.3.1 GRANITE FROM THE FEBEX TUNNEL (G-FEB).

Table 5 shows the summary of sorption experiments carried out with the FEBEX granite (*G-FEB*).

ROCK G-FEB	S/L ($g \cdot L^{-1}$)	WATER	EXPERIMENT	pH	[Cs] (M)
(F1)	50	LSW	Kin	6-7	$5.5 \cdot 10^{-9}$/ 10^{-9}-10^{-2}
(F2)	50	LSW	Kin	6-7	$5.5 \cdot 10^{-9}$/ 10^{-9}-10^{-2}
(F3)	50	LSW	Kin	6-7	$5.5 \cdot 10^{-9}$/ 10^{-9}-10^{-2}
(F1)	10	LSW	Edge/Iso	6-10	$5.5 \cdot 10^{-9}$
(F1)	10	HSW	Iso	6-7	10^{-9}-10^{-2}

Table 5. Summary of experiments with FEBEX granite (G-Feb). Kin=kinetic tests; Iso=Isotherms; Edge=Sorption edges

4.3.1.1 K_d measurements and kinetics on different fractions. [Cs] = $5.5 \cdot 10^{-9}$ M

These first sorption tests were carried out at a solid to liquid ratio of 0.5 g/ 10 mL (50 g/L), in LSW with pH between 6 and 7 trying to evidence the differences in the uptake kinetic considering the three different available fractions. The results for the F1 fraction were, in general, satisfactory, whereas the initial results for F2 and F3 fractions were not acceptable. In F2 and F3 fractions, despite of a first washing, lot of fines remained attached and their presence biased the experiments. This was clear during the centrifugation process. Thus, it was decided to wash carefully these fractions, for their use in further tests, and discard the first results obtained.

Thus, Figure 3 shows the cesium sorption kinetics obtained for F1, F2 and F3 fractions. The sorption onto the finest granite fraction (F1) did not show a significant kinetic, over a time span of approximately one year.

The mean $LogK_d$ measured for this fraction was 2.25 ± 0.07, even if the maximum error derived from sample heterogeneity was larger (around *0.16* in a log scale). In any case, it can be concluded that sorption values are all included within the range of $LogK_d$ between 2.1 and 2.4 approximately (i.e K_d between approximately 125 and 240 mL/g).

Cesium sorption in F2 and F3 fractions is slightly different. First, sorption kinetic is slower: more than 1 month is needed to reach the apparent sorption equilibrium. This is the first cause of the *spreading* of the experimental $LogK_d$ values, which now vary between 1.4 and 2.8 (K_d from 25 to 630 mL/g approximately).

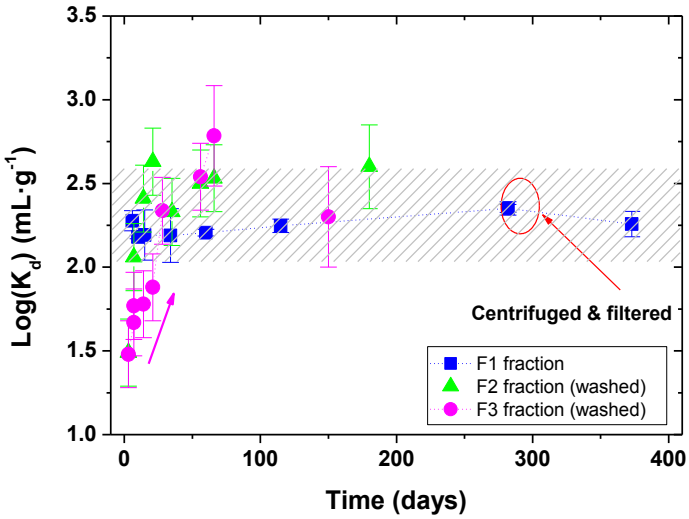

Figure 3. Kinetic of Cs adsorption in the three different fractions of the G-FEB granite.

If the data obtained before the apparent equilibrium is reached are not considered, the range is reduced to $logK_d$ between 2.2 and 2.8 (K_d from 160 to 630 mL/g). Nevertheless, it must be noticed that, when the size of the granite fraction increases, the experimental variation on the determined K_d values, due to sample heterogeneity, increases too. It is not clear however, why the mean K_d value at the equilibrium is slightly higher for the larger fractions. The hypothesis of poor centrifugation

for the finer fraction was assumed and thus one sample (rounded with a red circle in Figure 3) was centrifuged and filtered by 0.2 μm filter. However, the results were practically identical.

From these results the following conclusions can be drawn. (1) Cesium sorption kinetic is negligible for the finest sample used (<0.5 mm) whereas increases for the larger ones; at least one month is needed to reach the equilibrium. The equilibration time could be considered an additional cause of error in K_d determination above all when large rock fractions are used. Furthermore, increasing the material size fraction, the error due to the sample heterogeneity also increases, even if in this test, the final mean value is not very different. (2) Considering all the possible errors, including the heterogeneity of the material, the K_d values at the equilibrium for cesium in *G-FEB* granite range between 100 and 630 mL/g being the radionuclide concentration of [Cs] = $5.5 \cdot 10^{-9}$ M.

In order to limit the quantity of material used to perform sorption tests, we decided to make all the successive tests with a solid to liquid ratio 10 $g \cdot L^{-1}$ (0.1 g/ 10 mL). Thus, some K_d were determined with the F1 fraction, also at this solid to liquid ratio. The difference observed in the K_d obtained at the two different solid to liquid ratio were all within the experimental error.

4.3.1.2 Sorption Edges. [Cs] = $5.5 \cdot 10^{-9}$ M

The effect of pH has been evaluated using the same experimental conditions used for the kinetic tests. The F1fraction was used for these experiments and Table 6 summarizes the results obtained. A significant effect of pH on Cs sorption was not appreciated and all the K_d values fall within the previously mentioned range.

pH	K_d	$LogK_d$
3.52	148	2.171
6.13	176	2.245
7	160	2.190
7.9	160	2.205
9.3	137	2.137
Mean	**155 ± 14**	**2.19 ± 0.04**

Table 6. Cs distribution coefficients as a function of pH in the F1 fraction of G-FEB granite

4.3.1.3 Sorption Isotherms

The importance of radionuclide concentration on the magnitude of K_d values is well known, especially in the case of cesium, which presents non-linear sorption in many minerals. Micaceous minerals, in addition to *planar* sites in which exchange process usually take place, possess *frayed edge sites*, FES, arising from the weathering particles edges. Cations like Cs^+, Rb^+, Li^+, NH_4^+, K^+, are able to access these weathered edges whereas other bigger ions cannot. Thus, even FES density is very low they clearly dominate sorption at low Cs concentration (Missana et al., 2014).

Sorption isotherms were carried out, using the F1 fraction, and with pH fixed to 7.0 ± 0.2. The duration of the experiments was 14 days and cesium concentration, [Cs], varied from approximately

$2 \cdot 10^{-9}$ M to $1 \cdot 10^{-2}$ M. The solid to liquid ratio (S/L) was 10 $g \cdot L^{-1}$. Sorption isotherms were carried out both in the LSW and HSW (Table 5).

Figure 4 shows the comparison of Cs sorption isotherms in the *G-FEB (F1)* granite in the low and high saline waters, LSW and HSW. Data in Figure 4(a) are expressed as Log(K_d) *vs*. the logarithm of the Cs concentration at the equilibrium, Log(Cs_{FIN}). Data in Figure 4(b) are expressed as the logarithm of the Cs adsorbed, Log(Cs_{ADS}) *vs*. the logarithm of the Cs concentration at the equilibrium, Log(Cs_{FIN}). This double way of representing the sorption isotherms will be maintained in all the document.

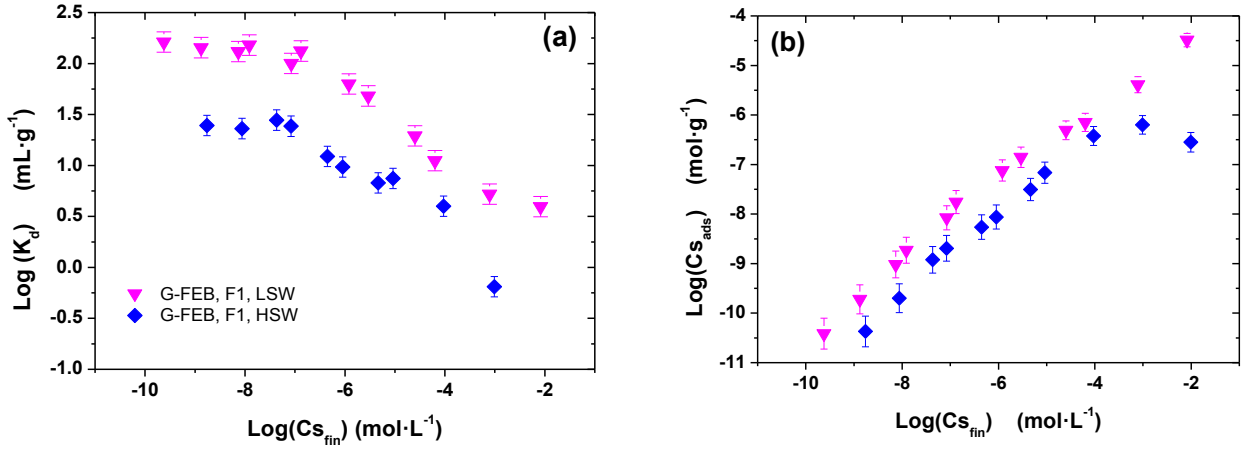

Figure 4. Cs sorption isotherms of G-FEB (F1) in (▲) low saline water, LSW, and (◆) high saline waters, HSW. (a) data expressed as LogK_d vs Log(Cs_{FIN}) and (b) data expressed as Log(Cs_{ADS}) vs Log(Cs_{FIN}).

From Figure 4 it can be observed that Cs sorption in *G-FEB* present a clear non-linear behavior. Linear sorption is observed at the lowest cesium concentrations, with a logK_d of 2.2 ± 0.1, in agreement with kinetic tests for LSW. When Cs concentration increases, clearly sorption decreases up to very small values (<5 ml/g).

In the case of sorption in HSW, a region with linear sorption is also observed with a logK_d of approximately 1.4 ± 0.1, being this maximum value (~25 ml/g) clearly lower than that measured in LSW. When the Cs concentration increases over $1 \cdot 10^{-8}$ M approximately, also in this case, K_d values start decreasing.

The effect of the ionic strength on cesium adsorption is evident when comparing the data obtained with the same material in LSW and HSW. Under saline conditions, cesium sorption is clearly lower. Under saline conditions, the variation of K_d, dependent on the cesium concentration, is from about 24 to 0.03 mL/g.

The progressive decrease in K_d values as concentration increases produce a variation of about one-two orders of magnitude. The radionuclide concentration probably represents one of the most important sources of variability in sorption data for Cs in these rocks.

4.3.2 RANITE FROM THE MIGRATION TUNNEL (G-MIG).

Table 7 shows the summary of all the sorption experiments carried out with the Migration granite (*G-Mig*).

ROCK G-FEB	S/L ($g \cdot L^{-1}$)	WATER	EXPERIMENT	pH	[Cs] (M)
G-Mig	10	LSW	Iso	6-7	$5.5 \cdot 10^{-9}/10^{-9}$-$10^{-2}$
bG-Mig	10	LSW	Iso	6-7	$5.5 \cdot 10^{-9}/10^{-9}$-$10^{-2}$
G-Mig	10	HSW	Iso	6-7	$5.5 \cdot 10^{-9}/10^{-9}$-$10^{-2}$
G-Mig	10	LSW	Edge	6.5-9.5	$5.5 \cdot 10^{-9}$

Table 7. Summary of experiments with the granite from the Migration tunnel (G-Mig). Iso=Isotherms; Edge=Sorption edges

4.3.2.1 Sorption Edges [Cs] = $5.5 \cdot 10^{-9}$ M

The effect of pH on Cs sorption has been evaluated in this rock using the LSW. Table 8 summarizes the results obtained. The measured values within the analyzed pH range are very similar within the expected experimental variation.

pH	Kd	$LogK_d$
6.55	940	2,973
7.91	1,153	3,062
8.12	990	2,995
9.2	1,127	3,052
Mean	**1,052 ± 103**	**3.02 ± 0.04**

Table 8. Distribution coefficients as a function of pH in the G-Mig granite

The mean logarithm of the distribution coefficient is approximately 3 ($K_d \sim 1000$ $mL \cdot g^{-1}$), almost one magnitude higher than that observed in *G-FEB* granite. The mineralogical composition or the different final water chemistry are most probably the reason why different K_d values are observed, as will be discussed later.

4.3.2.2 Sorption isotherms

The sorption isotherms with the *G-Mig* granite were carried out with the "standard" and the "black" one. Similar experimental conditions as used for the *G-FEB* granite were also applied: the pH was fixed to 7.0±0.2, the duration of the experiments was 14 days and [Cs] concentration varied from approximately $2 \cdot 10^{-9}$ M to $1 \cdot 10^{-2}$ M. The solid to liquid ratio was 10 $g \cdot L^{-1}$ (0.1 g/ 10 mL). The analysis of the effects of the ionic strength was carried out comparing the isotherms of the *G-Mig* in LSW and HSW. Tests with LSW were done with both (standard and black) rocks to compare their sorption behavior.

Figure 5 shows the sorption isotherms of Cs in low and high saline synthetic waters. As in the previous case, the effect of the ionic strength is relevant also for this rock, especially at low Cs concentrations (from $\log K_d$=3 to $\log K_d$= 2.5, for low and high saline waters respectively). As far as the concentration of Cs increases, the differences in sorption tend to disappear. The range of K_d variations for sorption in *G-Mig* in LSW is from about 1000 to 5 $mL \cdot g^{-1}$, whereas in HSW is from about 360 to 10 $mL \cdot g^{-1}$.

Figure 6 shows the experimental results obtained comparing the standard and black Grimsel granite in LSW. The K_d values are very similar in the two cases, except for very low Cs concentration, where sorption in the *black* rock seems to be higher (up to approximately 2000 mL·g-1. Using fine fractions, as those of *G-Mig* (<0.064 mm), the errors due to sample heterogeneity are negligible. This means that the possible differences in sorption due to the higher quantity of iron (or biotite) are limited to the region of low Cs concentrations.

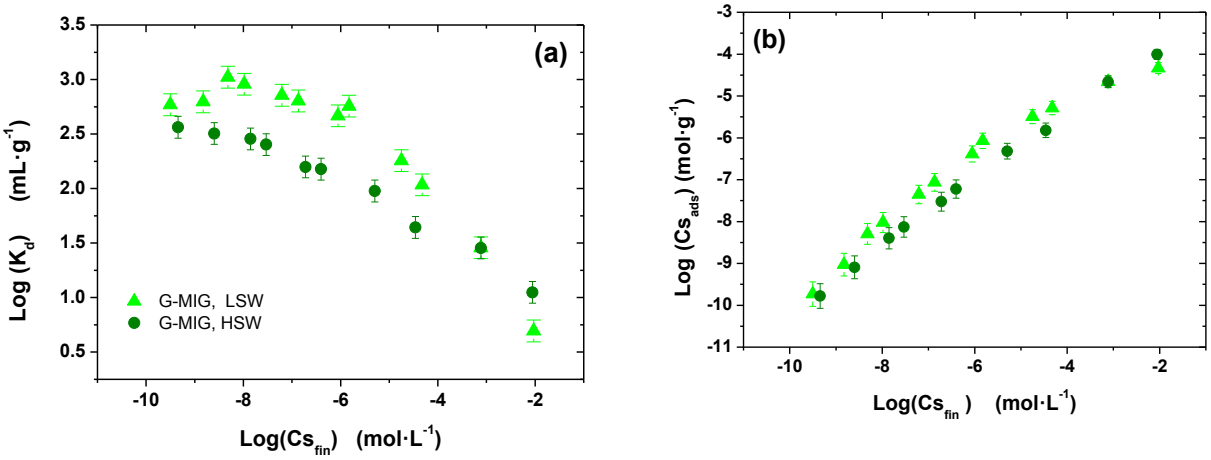

Figure 5. Cs sorption isotherms on G-Mig in (▲) low saline water, LSW and (●) high saline water, HSW. (a) data expressed as $LogK_d$ vs $Log(Cs_{FIN})$ and (b) data expressed as $Log(Cs_{ADS})$ vs $Log(Cs_{FIN})$.

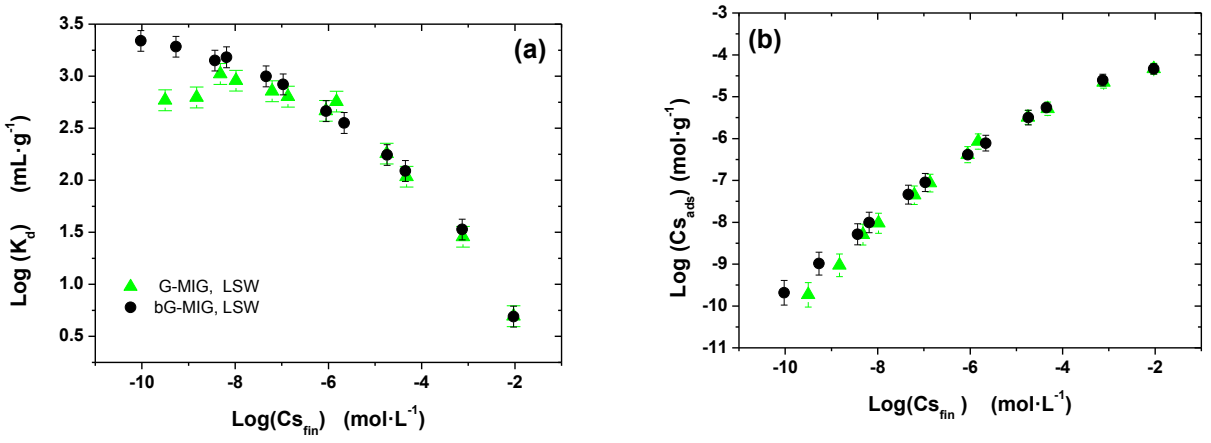

Figure 6. Cs sorption isotherms on (▲)G-Mig and (●) bG-Mig in low saline water, LSW (a) data expressed as $LogK_d$ vs $Log(Cs_{FIN})$ and (b) data expressed as $Log(Cs_{ADS})$ vs $Log(Cs_{FIN})$.

4.3.3 GRANITE FROM THE "LOS RATONES" MINE (RAT).

Table 9 shows the summary of the sorption experiments carried out the granite from *"Los Ratones"* mine (*Rat*). The granite coming from the SR-5 borehole was considered as the reference fresh material. Old K_d data obtained at CIEMAT, obtained as a function of the solid to liquid ratio, in different samples from different boreholes, taken from (García-Gutiérrez *et al.*, 200) are summarized in Table_A9. In old experiments the distribution coefficients were obtained using a Spanish commercial water which composition is shown in Table_A6. The new experiments were carried out with the reference (fresh) granite of this site (SR-5) in LSW.

Rock Rat	S/L ($g \cdot L^{-1}$)	WATER	TEST	pH	[I] (M)	[Cs] (M)
(SR-5)	1:10	LSW	Iso	6-7	$1 \cdot 10^{-3}$	10^{-9}-10^{-2}
(SR-5) OLD	1:10 -1:50	Commercial	K_d	7.5-8.5	$2 \cdot 10^{-3}$	$1 \cdot 10^{-7}$ - $1 \cdot 10^{-8}$
(SR-4) OLD	1:10 -1:50	Commercial	K_d	7.5-8.5	$2 \cdot 10^{-3}$	$1 \cdot 10^{-7}$ - $1 \cdot 10^{-8}$
(SR-3) OLD	1:10 -1:50	Commercial	K_d	7.5-8.5	$2 \cdot 10^{-3}$	$1 \cdot 10^{-7}$ - $1 \cdot 10^{-8}$
(SR-2) OLD	1:10 -1:50	Commercial	K_d	7.5-8.5	$2 \cdot 10^{-3}$	$1 \cdot 10^{-7}$ - $1 \cdot 10^{-8}$
(SR-1) OLD	1:10 -1:50	Commercial	K_d	7.5-8.5	$2 \cdot 10^{-3}$	$1 \cdot 10^{-7}$ - $1 \cdot 10^{-8}$

Table 9. Summary of experiments with Rat granite. Iso=Isotherms

4.3.3.1 Sorption Isotherms

Figure 7 shows the results of the sorption isotherms obtained with the *Rat* granite (SR-5) in LSW. As observed in the previous crystalline rocks analyzed, Cs sorption is not linear as the distribution coefficients clearly decrease as the radionuclide concentration increases.

$LogK_d$ values are all included within the range between 3 and 0.6 approximately (i.e K_d between approximately 1000 and 4 mL/g). These measured values are totally comparable with those obtained with the *G-Mig* granite under the same experimental conditions and the most important source of variability in K_d values is Cs concentration.

4.3.3.2 Comparison with previous sorption tests: K_d measurements. [Cs] = $1.1 \cdot 10^{-7}$-$1.1 \cdot 10^{-8}$ M

Old sorption tests were carried out on all the samples from different five boreholes from *Los Ratones* mine. The description of the analyzed samples is detailed in TableA_3; furthermore, all the K_d obtained are summarized in Table A 9 of the Annex.

The mean K_d values ranged from approximately 330 to 3500 mL/g, (2.51-3.55) for cesium concentration about $1 \cdot 10^{-7}$ - $1 \cdot 10^{-8}$ M. It can be deduced that there is a substantial variability which can be attributed to the heterogeneity of the material and the different degree of alteration of the samples.

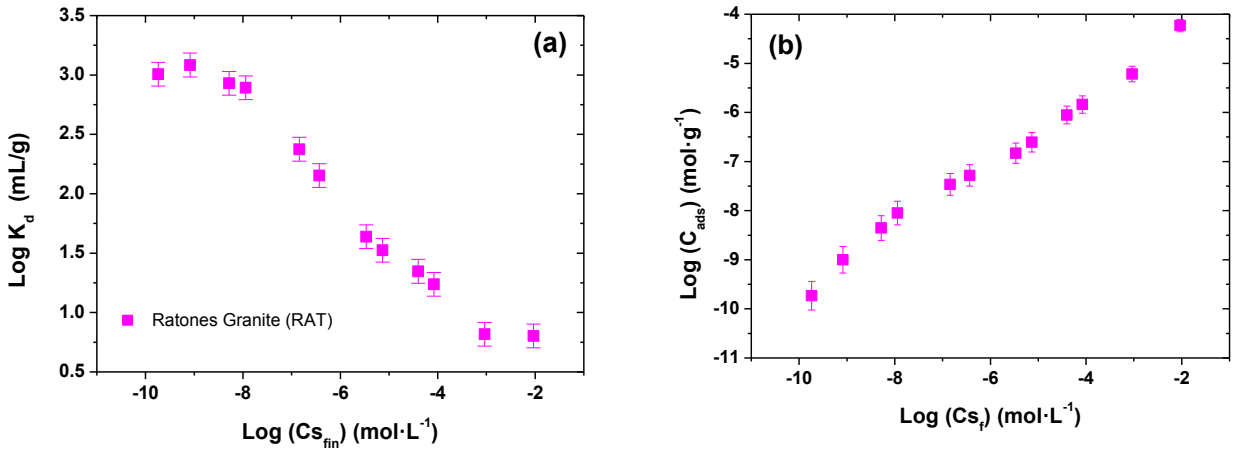

Figure 7. Cs sorption isotherms on Rat granite in low saline water, LSW. (a) data expressed as LogK_d vs Log(Cs_{FIN}) and (b) data expressed as Log(Cs_{ADS}) vs Log(Cs_{FIN}).

Some of the variation can be also attributed to the different experimental conditions (tests were carried out at different solid to liquid ratios) as, in fact, a slight dependence on the solid to liquid ratio used is detected, the less the solid the high the K_d values used.

Considering all the available values the mean K_d for the *Perdices* type granite was 1344 ± 560 mL/g (LogK_d = 3.13), not very different from the values obtained for the *Cabeza Porquera* type (1529 ± 860 mL/g, LogK_d=3.18).

The summary of the old data related to the SR-5 reference sample, obtained at the solid to liquid ratio of 10g/L and thus comparable to the new ones (Figure 7) is presented in Table 10. The "old" K_d values obtained under similar experimental conditions of Cs concentration correspond quite well with the new data.

Sample	$K_{d\ (ml/g)}$	LogK_d
SR5-CIE-MS-1	**904**	**2.96**
SR5-CIE-MS-2	**1,516**	**3.18**
SR5-CIE-MS-3	995	2.98
SR5-CIE-MS-4	1,293	3.11
SR5-CIE-MS-5	2,062	3.31

Table 10. K_d data extracted from Table A9 for SR-5 samples. [Cs]=2.1·10^{-8} M.

4.3.4 GRANITE FROM THE "EL BERROCAL" (BER).

Table 11 shows a summary of all the sorption experiments carried out with the granite coming from El Berrocal (*Ber)*. In the Table old experiments carried out by CIEMAT in previous projects (Garcia-Gutiérrez, 1994) have been also added.

Rock Rat	S/L ($g \cdot L^{-1}$)	WATER	TEST	pH	[I] (M)	[Cs] (M)
Ber	10	LSW	Isotherms	6-7	$1 \cdot 10^{-3}$	10^{-9}-10^{-2}
Ber	10	HSW	Isotherms	6-7	$1 \cdot 10^{-3}$	10^{-9}-10^{-2}
W-Ber	10	LSW	Isotherms	6-7	$1 \cdot 10^{-3}$	10^{-9}-10^{-2}
BER OLD	20	Natural (S2)	Kinetic	8	$1 \cdot 10^{-3}$	10^{-9}-10^{-3}

Table 11. Summary of experiments with El Berrocal granite

4.3.4.1 Sorption isotherms

Figure 8 shows the results of the Cs sorption isotherms obtained with the fresh granite from the "El Berrocal" (*Ber*) in LSW and HLW.

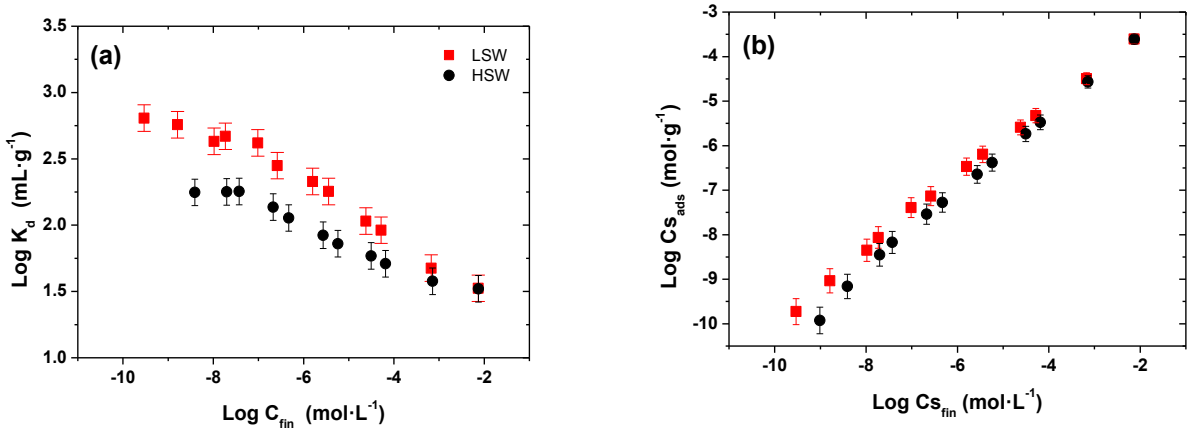

Figure 8. Cs sorption isotherms on the fresh Ber granite in: (■) LSW and (●) HSW. (a) data expressed as LogK_d vs Log(Cs_{FIN}) and (b) data expressed as Log(Cs_{ADS}) vs Log(Cs_{FIN}).

Once again, Cs sorption is not linear, and clearly decreases as the radionuclide concentration increases with a larger variation in LSW than HSW. For LSW sorption values are all included within the range of LogK_d between 2.8 and 1.6 approximately (i.e K_d between approximately 650 and 40 mL/g) whereas in the case of of HSW, K_d values are lower and vary from approximately 160 and 40 mL/g. Also in this case, the ionic strength plays a role on Cs sorption, more evident at low Cs concentration.

As already mentioned, the alteration degree of a rock may affect its sorption properties, for this reason, it is interesting to compare the fresh material to the weathered one. Figure 9 shows the Cs sorption isotherms obtained with the *Ber* granite from the S15 borehole, corresponding to a zone of weathered rock, compared to that of the borehole S16, which can be considered the fresh reference, material.

At low Cs concentrations, the weathered rock present clearly higher sorption than the fresh granite (LogK_d ~ 4.0 *vs* LogK_d ~2.8) and the difference tends to decrease when cesium concentration increases. The higher sorption observed would agree with the significant increase in the BET surface area upon the weathering but, in any case, Cs concentration still determines the minor/mayor relevance of the weathering on sorption.

4.3.4.2 Comparison with previous sorption tests: kinetic measurements. [Cs] = $1.1 \cdot 10^{-9}$ to $1.1 \cdot 10^{-3}$ M

The water used in the old tests with El Berrocal reference granite (S-16), was a natural granite water coming from the site (S2 borehole), whose composition is detailed in Table_A6. The rock was crushed in an agate mortar and sieved at 0.5 mm; the solid to liquid ratio was 20 g/L and the pH was approximately 8. The solid was separated from the aqueous phase by centrifugation (8000 rpm, 20 min). K_d values were obtained as a function of time and initial Cs concentration. These results are summarized in Table 12.

[Cs] (M)	1 week	2 weeks	4 weeks	6 weeks	8 weeks
$1 \cdot 10^{-3}$	0.9 (-0.05)	1.1 (0.04)	1.5 (0.18)	3.3 (0.52)	4.2 (0.62)
$1 \cdot 10^{-5}$	12.8 (1.11)	16.2 (1.21)	19.8 (1.30)	23.5 (1.37)	23.3 (1.37)
$1 \cdot 10^{-7}$	153.1 (2.18)	214.7 (2.33)	324.7 (2.51)	362.3 (2.56)	342.6 (2.53)
$1 \cdot 10^{-9}$	281.5 (2.45)	399.1 (2.60)	567.7 (2.75)	897.8 (2.95)	506.8 (2.70)

Table 12. Kd values obtained in old adsorption experiments with Ber (reference granite from S-16 borehole).

The comparison of the data from the present study (Figure 8) with the old ones (obtained after two weeks) shows that K_d values are quite similar, despite the experimental differences between the new and old sets of data (water, solid to liquid ratio and centrifugation time). It has to be mentioned that in the old experiments, carried out with a grain size of 0.5 mm, the time needed to reach the equilibrium was approximately 1 month.

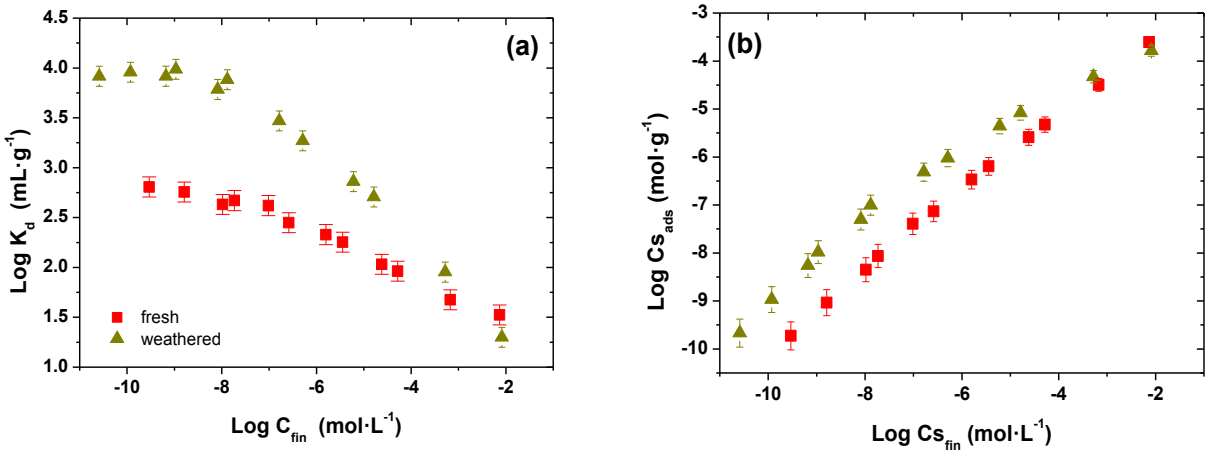

Figure 9. Cs sorption isotherms on (▲)weathered Ber granite compared to the (■) fresh one in LSW. (a) data expressed as LogK_d vs Log(Cs_{FIN}) and (b) data expressed as Log(Cs_{ADS}) vs Log(Cs_{FIN}).

4.3.5 GRANITE FROM ÄSPÖ HARD ROCK LABORATORY (ÄS).

Table 13 shows a summary of the sorption experiments carried out with the Äspö diorite. No previous data on this rock were available at CIEMAT. All these tests were performed under anoxic conditions to preserve the properties of the recently drilled material.

Rock Äs	S/L ($g \cdot L^{-1}$)	WATER	TEST	pH	[I] (M)	[Cs] (M)
Äs-f	10	Synt Äspö	Kin	6-7	$1 \cdot 10^{-1}$	10^{-9}
Äs-g	10	Synt Äspö	Kin	6-7	$1 \cdot 10^{-1}$	10^{-9}
Äs-f	10	Synt Äspö	Edge	6.5-9	$1 \cdot 10^{-1}$	10^{-9}
Äs-g	10	Synt Äspö	Edge	6.5-9	$1 \cdot 10^{-1}$	10^{-9}
Äs-f	10	Synt Äspö	Iso	6-7	$1 \cdot 10^{-1}$	10^{-9}-10^{-2}
Äs-g	10	Synt Äspö	Iso	6-7	$1 \cdot 10^{-1}$	10^{-9}-10^{-2}

Table 13. Summary of experiments with Äspö granite. Kin= Kinetics; Iso=Isotherms; Edge=Sorption edges

4.3.5.1 K_d measurements, kinetics. [Cs] = $5.4 \cdot 10^{-9}$ M

The first experiments have been carried out with both the fractions of the Äspö granite, to evaluate the kinetic of Cs adsorption (Figure 10) and the synthetic Äspö water was used. The K_d values were not very different, even if the time needed to reach the equilibrium was slightly higher in the sample with the larger grain size.

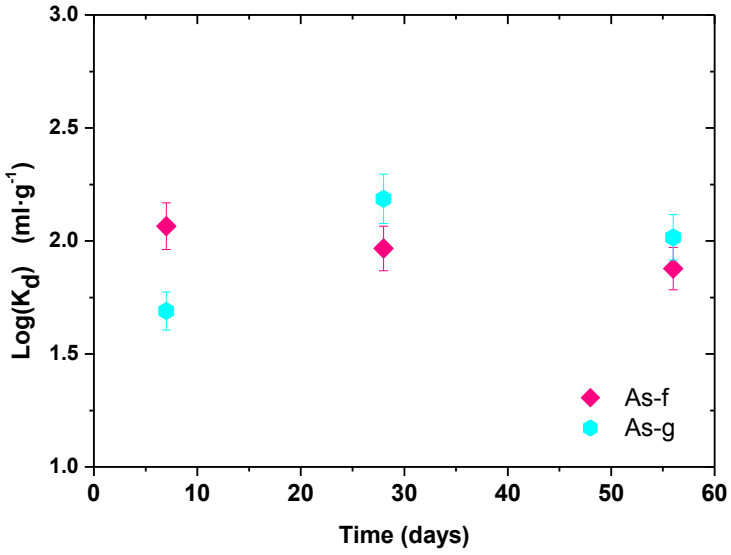

Figure 10.Cs sorption kinetics in the Äspö granite: (◆) fine and (●) gross).

However, the difference between the two samples are within the experimental error. The K_d obtained for this Cs concentration is approximately 100 ml/g.

4.3.5.2 Sorption Edges. [Cs] = $5.3 \cdot 10^{-9}$ M

The effect of pH on Cs sorption in the rock from Äspö has been evaluated using the same experimental conditions used for the kinetic tests. Table 14 summarizes the results obtained.

No large differences were observed with pH for Cs sorption onto Äspö rock; furthermore, as observed in Figure 10 there are not significant differences of K_d values between the fine and gross fraction, being the mean K_d values for the fine and gross fractions are 96 and 117 ml/g respectively ($LogK_d$ approximately 2) at low Cs concentration. However, the data are much dispersed in the case

of the gross fraction, as already observed for the *G-FEB*. These relatively low K_d values are due to the salinity of the Äspö synthetic water.

SAMPLE	pH	K_d	LogKd
Äs-f	6.31	105.82	2,025
Äs-f	5.99	83.77	1,923
Äs-f	7.69	94.67	1,976
Äs-f	8.57	98.23	1,992
	Mean K_d	**96±9**	**1.98±0.04**
SAMPLE	**pH**	**K_d**	**LogKd**
Äs-g	6.3	57.12	1,757
Äs-g	6.07	179.53	2,254
Äs-g	7.59	143.15	2,156
Äs-g	8.65	87.53	1,942
	Mean K_d	**117±55**	**2.03±0.22**

Table 14. K_d values as a function of pH in the Äspö rock (fine and gross)

4.3.5.3 Sorption isotherms

Sorption isotherms were carried out with fine and gross Äspö diorite in the synthetic Aspö water; the duration of the experiments was 14 days and the concentration of the radionuclide varied from approximately $2 \cdot 10^{-9}$ M to $1 \cdot 10^{-2}$ M.

The results of these tests are plotted in Figure 11. K_d values span from approximately 100 to 30 ml/g in the fine fraction (Äs-f) and from 100 to 5 mL/g in the large one (Äs-g). The difference between fine and gross fractions seems to be accentuated at high Cs concentration, even if it must be accounted that when K_d are lower than 10 mL/g, the experimental error increases, thus this difference may not be very significant.

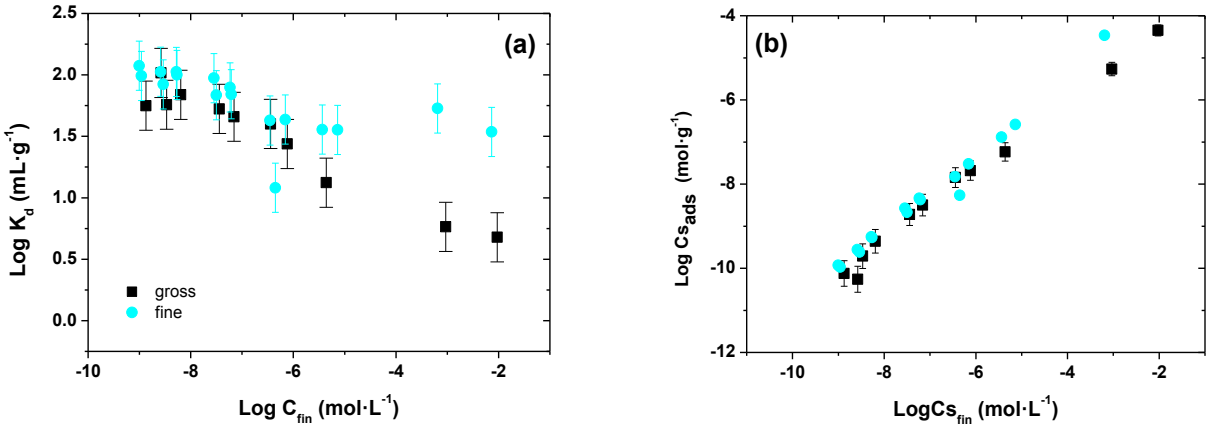

Figure 11.Cs sorption isotherms on Äspö granite (●) fine and (■) gross in synthetic Äspö groundwater. (a) data expressed as LogK_d vs Log(Cs_{FIN}) and (b) data expressed as Log(Cs_{ADS}) vs Log(Cs_{FIN}).

4.4 COMPARISON OF SORPTION DATA FROM DIFFERENT CRYSTALLINE ROCKS

In the following sections, the data obtained in different rocks under the same experimental conditions will be compared to facilitate the discussion the obtained results. In order to better evaluate the effects produced by the variation of the radionuclide concentration in the non-lineal behavior observed, the comparison of data will be carried out with the sorption isotherms. Data will be expressed as the logarithm of the distribution coefficient, K_d, as a function of the logarithm of the cesium in the aqueous phase at the equilibrium ($LogCs_{fin}$).

4.4.1 CESIUM SORPTION IN LOW SALINE WATERS

Figure 12 shows the comparison of all the data obtained with the low saline water, LSW. As commented in the previous sections, Cs sorption is clearly not linear in all the solids investigated. As cesium can exists in the aqueous phases mainly in the form of monovalent Cs^+, the non-linearity in sorption can only be attributed to the existence of different sorption sites with different density and affinities for this ion. This behaviour is quite common for Cs in micaceous minerals, as already mentioned.

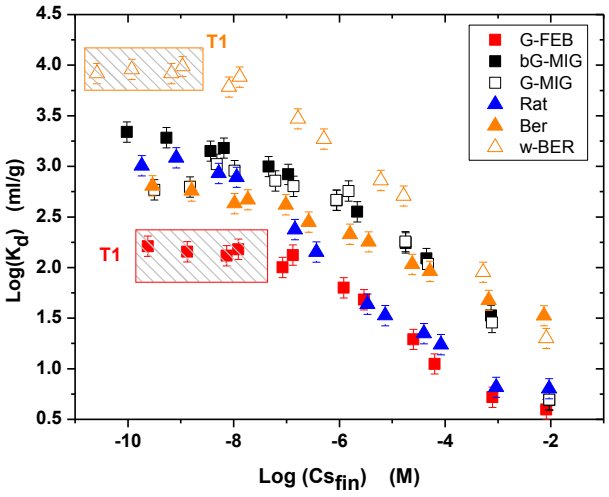

Figure 12.Comparison of Cs sorption isotherms obtained in different crystalline rocks with LSW.

The quantity of the first type of sites, that will be denominated "strong" sites (T1), can be determined from shape of the isotherms (see Figure 12). In these strong sites, which dominates sorption at very low concentrations, sorption is linear (K_d does not vary with concentration). T1 sites present low capacity but very high affinity for Cs (K_d values are the highest). These sites can be related to frayed edge sites (FES), present in micas materials, where only cations Cs^+, K^+, Rb^+, Li^+ NH_4^+ can have access.

The saturation of these sorption sites is clearly observed because K_d values start decreasing significatively when Cs concentration overcomes $1{\cdot}10^{-8}$ - $1{\cdot}10^{-7}$ M. At higher Cs concentrations, sorption must be controlled by, at least, an additional sorption site or "weak site". However, in

different micaceous materials, as illite, the sorption behaviour of Cs, has been modelled using a three-sites approach (Bradbury& Baeyens, 2000; Muuri et al., 2017).

Considering the variation of K_d values for the same material, the mayor spreading is due to the radionuclide concentration (from 1 to 2.5 orders of magnitudes depending on the solid, Figure 12).

As shown in Figure 12, the weathered rock (*w-Ber*) shows the highest sorption capacity at any Cs concentrations, and this can be explained by its surface area, which is significantly higher than that of any other fresh rock.

Considering the rest of *fresh* rocks, the variation of K_d values at low Cs concentration ([Cs]<$1 \cdot 10^{-7}$ M) is about one order of magnitude. The *G-FEB* shows the lowest adsorption, whereas the *black G-Mig* shows the highest one. The others (*Rat, Ber* and *G-Mig*) show similar K_d values within the experimental error.

When Cs concentration increases, sorption data are very similar for *G-Mig*, b*G-Mig* and *Ber*, which are one order of magnitude higher than those of *G-FEB* and *Rat*, which are very similar between them. The first three mentioned rocks have higher BET surface areas (3-4 m^2/g) than the last two (0.1-0.5 m^2/g), which is a factor to be accounted for in the analysis of data.

To analyze the effect of the surface area on the sorption data, it is of interest plotting the sorption isotherms considering the K_d values "normalized" to the BET surface area, as shown inFigure 13.

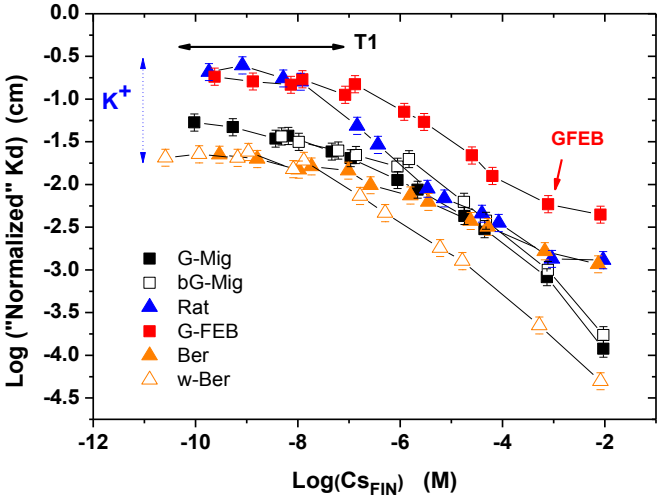

Figure 13.Comparison of Cs sorption isotherm obtained in different crystalline rocks with LSW, showing K_d values normalised to the BET area of each sample.

When the distribution coefficients are normalized to the BET area, it can be observed as the weathered *Ber* rock at medium – higher loading is the one presenting less relative adsorption capacity. For the fresh rocks, the differences in sorption capability are all contained within one order of magnitude, with the largest variations observed at low Cs loadings. At medium-high concentrations, the differences in Log (K_d) are small, being the values very similar for all the granites, being the *G-Feb* the only exception.

The differences observed at low Cs concentrations, where sorption is dominated by the "strong" sites, could be related to the presence of potassium (or any other competitive ion) in solution.

Sorption data normalised to the BET area, shown in Figure 13, indicate that Cs is adsorbed in the following order: *Rat* ≈ *G-Feb* > *G-Mig*> *Ber*. This sequence nicely agrees with the inverse aqueous content of potassium shown in Table 4.

In addition, Figure 13 shows that at medium-high Cs loadings, the normalized sorption values are very similar in all the investigated fresh rocks, with the exception of the *G-Feb* granite. The *G-Feb* sample shows slightly higher relative adsorption capacity than the rest, and the shape of the isotherm is also different. This could be related to chemical/mineralogical differences between this rock and the others.

Missana & García-Gutiérrez (2014) analysed the adsorption behaviour of Cs in three different granite minerals: biotite, muscovite and potassium feldspar, FdK. The Cs sorption isotherms of these minerals are reported in Figure 14 where data are already normalised to their BET surface area, to compare these data to those shown in Figure 13.

Figure 14 shows that Cs sorption is not linear in all the minerals investigated, as expected, and that at medium-high loadings the normalized sorption values are quite similar. For what concerns the difference observed at low Cs concentration, again the mayor source of variability could be attributed to the quantity of aqueous K^+ ($1.5 \cdot 10^{-5}$ M for the muscovite, $8.5 \cdot 10^{-5}$ for the biotite and $3.3 \cdot 10^{-4}$ for FdK).

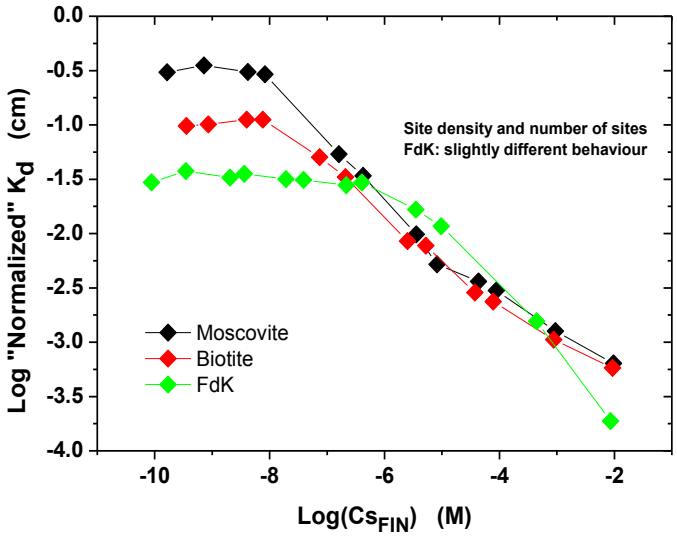

Figure 14.Cs sorption isotherms in different granite minerals: muscovite, biotite y FdK in LSW (10g/L). K_d data are normalized to the BET surface area.

Furthermore, the shape of the Cs isotherm on FdK is clearly different from that of other two minerals. Apparently, the density of T1 sites is higher in FdK than in the other minerals. Thus, the slight differences observed in the isotherms of *G-Feb* granite with respect to the others might be caused by its highest FdK content (31-37 %).

4.4.2 CESIUM SORPTION IN HIGH SALINE WATERS

Figure 15 shows the sorption isotherms of cesium onto three different granites in high saline waters. HSW was used for *G-FEB* and *G-Mig* and *Ber*, whereas the Äspö synthetic water was used for the Äspö granite (*Äs*). As observed in the previous paragraphs, the salinity of the water is important for cesium adsorption, because in general it tends to decrease the Cs retention.

Under saline conditions the highest sorption is observed for the *G-Mig* and *Ber* rocks, which present slightly higher BET surface area than the other two. Therefore, to analyze which are the additional parameters that can affect sorption K_d data were normalized to the BET surface area and the results are plotted in Figure 16.

Once normalized to their BET area, the difference between the materials are not very large (within an order of magnitude) but they are clearly ordered according to the following order: *Äspö* > *G-FEB*>*G-Mig* =*Ber.* It is not very clear if the mineralogy of the material is relevant at such high ionic strength, but it can be noted that the Äspö diorite is the material that has the highest quantity of biotite and the lowest of quartz.

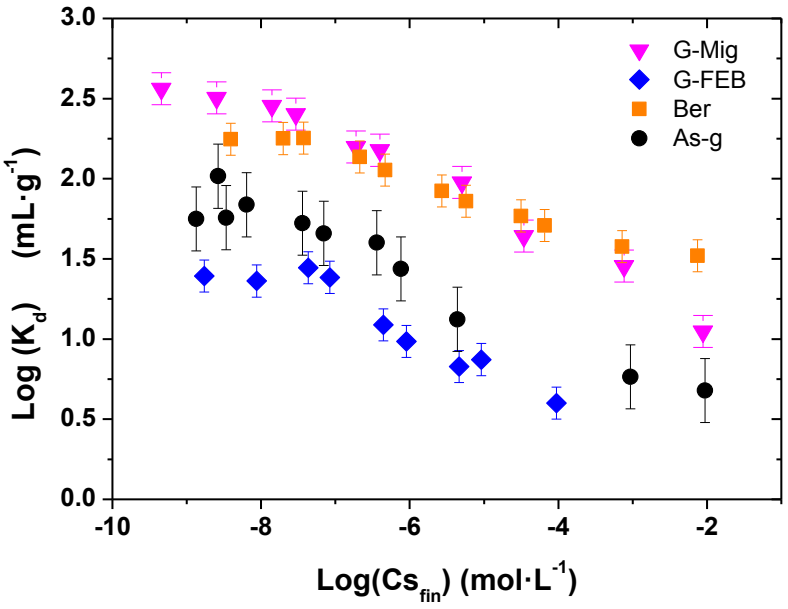

Figure 15.Comparison of sorption isotherm of Cs obtained in different crystalline rocks and HSW or Äspö synthetic groundwater.

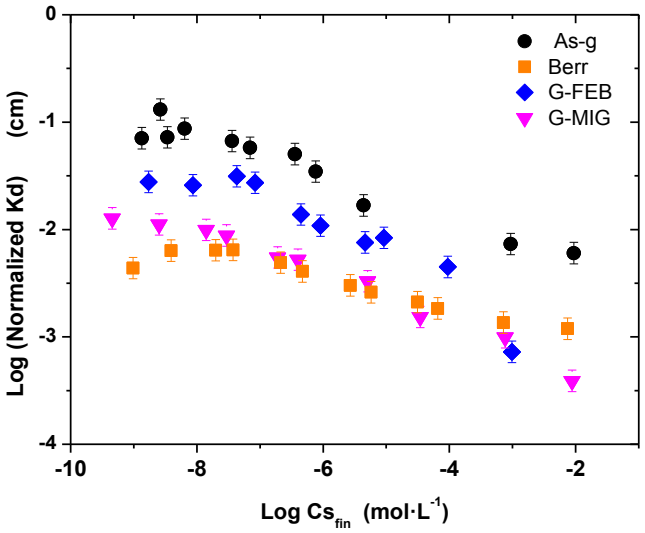

Figure 16.Comparison of sorption isotherm of Cs obtained in different crystalline rocks and HSW or Äspö synthetic groundwater. K_d data normalised to the BET surface area.

5 MODELLING

In a first instance, the objective of the modelling of data described so far is to catch the main factors that affect Cs adsorption in crystalline rocks. At this stage, the modelling is not expected to be "mechanistic", because a more detailed study on sorption by component minerals would be necessary, but it must be detailed enough to quantify the effects of the principal causes of variability of Cs distribution coefficients observed.

To start with the development of the sorption model the following important points will be considered:

1. Cs adsorption depends on the ionic strength of the water, but it is almost independent on pH.

2. Cs adsorption is non lineal.

Thus, the most probable sorption process of Cs sorption in crystalline rocks is cationic exchange and due to non-linearity of the process, more than one sorption site must be considered.

This first simplified modelling approach considers the existence of monovalent exchange, including at least 2 sites. The concentration of the strong sites (T1) can be estimated observing at which adsorbed Cs concentration the sorption isotherm starts bending (0.1-1 $\mu eq/m^2$); the concentration of other weaker sites, which acts when the Cs concentration is intermediate, cannot be always straightforwardly determined, but it can be obtained by the fit of the isotherm shape. In this study, we fixed the possible range of this site contribution (T2) between 3 and 5 $\mu eq/m^2$. The last and weakest site (T3) density can be determined by the total CEC of the sample; this value is not the same for all the rocks analyzed, but it can be fixed to approximately 1 meq/100 g. The retention in these last sites is in general quite low and often their contribution can be neglected.

The analysis of the experimental data showed that the extent of sorption depends on the BET surface area of the material, but also that when the data are normalized to this value, the mayor differences are observed at low Cs concentrations (in T1 sites) and that are probably due to the presence of competitive ions. Thus, the competitive effect of K^+ in Cs sorption must be accounted for, because it represents an important source of uncertainty in K_d values.

As previously mentioned, it is interesting to go more in depth to the contribution of constituent minerals on the overall sorption, for a more precise description of sorption processes. For example, based on the data obtained so far, it can be deduced that the presence of potassium feldspar (FdK) can be a factor of importance in Cs retention.

Especially the presence of FdK, for its content in potassium, seems to generate a different type of T1 sites (less selective and with higher concentration) in respect to the other minerals. The shape of the Cs isotherm on FdK, is in fact significantly different from that of the other two analyzed minerals (Figure 14) as the shape of the *G-FEB* (which contains the high quantity of Fdk) is different from the other crystalline rocks.

In summary, the performed modelling must be able to reproduce the sorption behavior of Cs particularly its dependence on Cs concentration, salinity and potassium content in the water. In the following paragraphs the modelling performed for those rocks in which we have more information (data performed in both LSW and HSW) will be described.

In the following Figures some examples of the fits obtained for the Cs sorption isotherms in different granites are shown. Table 15 shows the summary of the selectivity coefficients used to model the sorption isotherms, under different chemical conditions (LSW, HSW or Äspo synthetic water) and the value of the aqueous potassium, which is the main competitive ion.

It is interesting noting that the parameters needed for the same material under different experimental conditions (for example for *G-FEB* and *G-Mig*) are very similar within the expected errors.

SAMPLE	**K^+ (mol/l)**	**Site 1 (T1) $LogK_{SEL}$**	**Site 2 (T2) $LogK_{SEL}$**	**Site 3 (T3) $LogK_{SEL}$**
G-FEB, LSW	8.5E-05	8.35	4.75	-0.65
G-FEB, HSW	2.0E-04	8.20	4.50	-0.65
Mean (G-FEB)		**8.28±0.08**	**4.63±0.13**	**-0.65±0.0**
SAMPLE	**K^+ (mol/l)**	**Site 1 (T1) $LogK_{SEL}$**	**Site 2 (T2) $LogK_{SEL}$**	**Site 3 (T3) $LogK_{SEL}$**
G-Mig, LSW	2.5E-04	7.40	3.25	---
G-Mig, HSW	2.5E-04	7.25	3.05	---
bG-Mig, LSW	2.6E-04	7.25	3.05	---
Mean (G-Mig)		**7.30±0.10**	**3.12±0.13**	
SAMPLE	**K^+ (mol/l)**	**Site 1 (T1) $LogK_{SEL}$**	**Site 2 (T2) $LogK_{SEL}$**	**Site 3 (T3) $LogK_{SEL}$**
Rat, LSW	5.4E-05	8.3	2.8	-1.5
ÄsG, Synt Wat	5.4E-04	8.5	5.0	1.8

Table 15. Summary of the parameters used for modelling the sorption isotherms

Figure 17 to Figure 21 shows the experimental data and the model obtained with parameters included in Table 15; the model is superimposed to the experimental data as a continuous line. In particular, Figure 17 shows the modelling of the data of *G-FEB* in LSW and HSW; Figure 18 the data of *G-Mig* in LSW and HSW; Figure 19 the data of *bG-Mig* in LSW; Figure 20 the data of *Rat* in LSW and, finally, Figure 21 the data of *Äs-g* in synthetic Äspö water.

As can be seen in al the Figures, this simple model is able to reproduce quite satisfactorily in all the cases the main source of variability of Cs distribution coefficients in crystalline rocks, namely: radionuclide concentration, ionic strength of the water (and pH) as well as the presence of the main competitive ion, potassium.

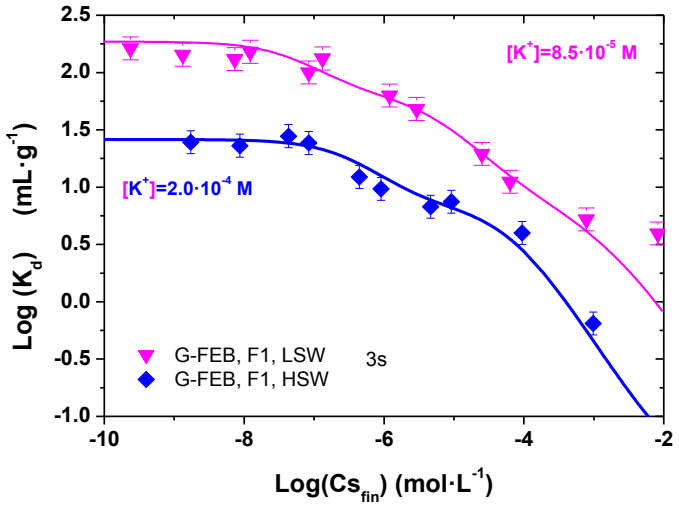

Figure 17.Modelling of the Cs sorption isotherms obtained in G-FEB in LSW and HSW waters

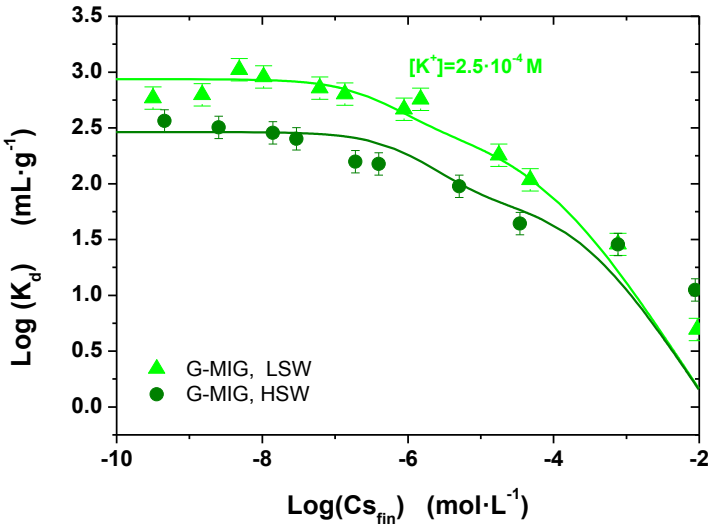

Figure 18.Modelling of the Cs sorption isotherms obtained in G-Mig in LSW and HSW waters

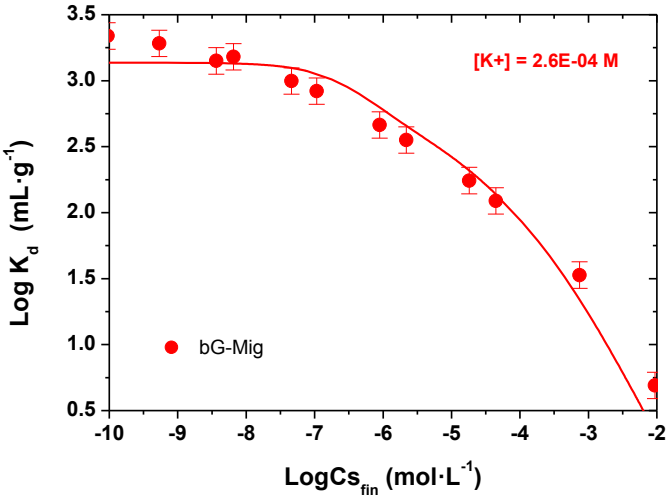

Figure 19.Modelling of the Cs sorption isotherms obtained in bG-Mig in LSW.

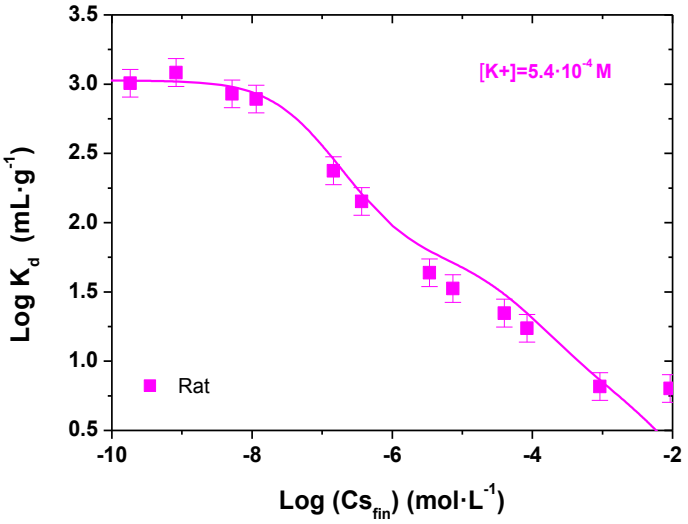

Figure 20.Modelling of the Cs sorption isotherms obtained in Rat in LSW.

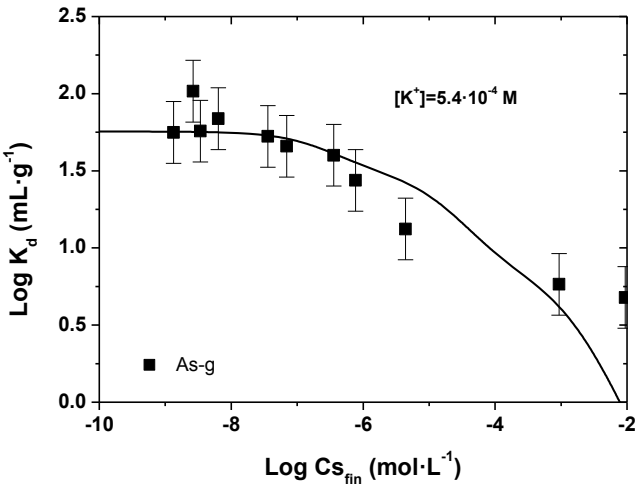

Figure 21.Modelling of the Cs sorption isotherms obtained in Äs-g in Äspö synthetic water..

6 HETEROGENEITY AND UP-SCALING

It has been shown in the previous section that simple models can be very useful to calculate the distribution coefficient of cesium for different minerals under different conditions. Despite of the large diversity of the materials used and their intrinsic heterogeneity, if the tests are carried out under similar experimental conditions, for a given Cs concentration the variability is restricted within approximately one order of magnitude. A more mechanistic treatment of the mineralogical heterogeneity can be done studying the sorption behavior on the main component of the rock, evidencing the main sorption properties and concentration of each one. For sure, the analysis of retention processes by batch experiments and their modelling is necessary for the understanding of the mechanisms involved in retention.

However, one of the main issues in the treatment of sorption processes in crystalline rocks is how K_d values obtained from batch laboratory experiment (usually made with crushed materials) can be extrapolated to field conditions. In general, literature data reports that crushed materials typically have sorption surface areas 10–100 times larger than that of the intact rock and that K_d values obtained in crushed rocks depend on the selected size and always overestimate those obtained with the intact rock (André et al., 2008).

The reasons why this can occur may be different and be related or not to "experimental" (unavoidable) problems. It must be considered that when the material is crushed, pores that in the intact material were not accessible, can be opened and fresh reactive surfaces created, this leading to higher surface area. For this reason, is always important to analyze the relationship between K_d values and surface area.

It would be nice to measure K_d and BET in different fractions and to extrapolate the distribution coefficient to *in-situ* conditions, unfortunately this procedure in crystalline rocks is not always effective, as fractionation of different minerals in different size fractions may occur.

In any case, the normalization of K_d values through the BET (which lead to the surface distribution coefficient, K_a) is a good starting point to evaluate the distribution coefficients in "realistic" conditions or at least to perform conservative assumption on the selection of K_d for performance assessment.

The use of coupons of intact rocks instead of crushed material to study retention properties of crystalline rocks is now more frequently proposed (André *et al*., 2009; Alonso *et al.*, 2014), but also in this case, several issues must be considered.

Probably the most important point is related to the kinetic of the sorption process. Fom batch sorption experiments it was observed that the larger the size fraction, the larger the time needed to reach the sorption equilibrium. To determine a valid distribution coefficient, it is necessary to ensure that the equilibrium is actually reached.

When working with coupons of crystalline rocks (even if they are relatively small) the time needed to reach the equilibrium may be extremely large for a direct experimental evaluation. As an example, Figure 22 shows the comparison of the distribution coefficients obtained for cesium ($[Cs]=1\cdot10^{-9}$ M) in a granitic rock in the powdered material and in a small block of the same

materials (right part of the Figure). In both cases, the water in contact with the solids was the same and the solid to liquid ratio very similar.

In the powdered rock, the equilibrium was reached in a few days, whereas the distribution coefficient measured in the small block was still increasing after more than 300 days. Additionally, the K_d obtained in the crushed rock (~140 $g \cdot mL^{-1}$) was almost one order of magnitude higher than the maximum obtained in the small piece of rock (~33 $g \cdot mL^{-1}$).

Indeed, this comparison might not be significative if both values are not taken at the equilibrium. To perform sorption experiments in wide range of experimental conditions to feed mechanistic models might be an unaffordable work if coupons are used.

Furthermore, the errors on K_d determination are larger when the grain size is larger, due to the intrinsic heterogeneity of these materials. Therefore, the use of small blocks is expected to introduce larger intrinsic errors on K_d determinations.

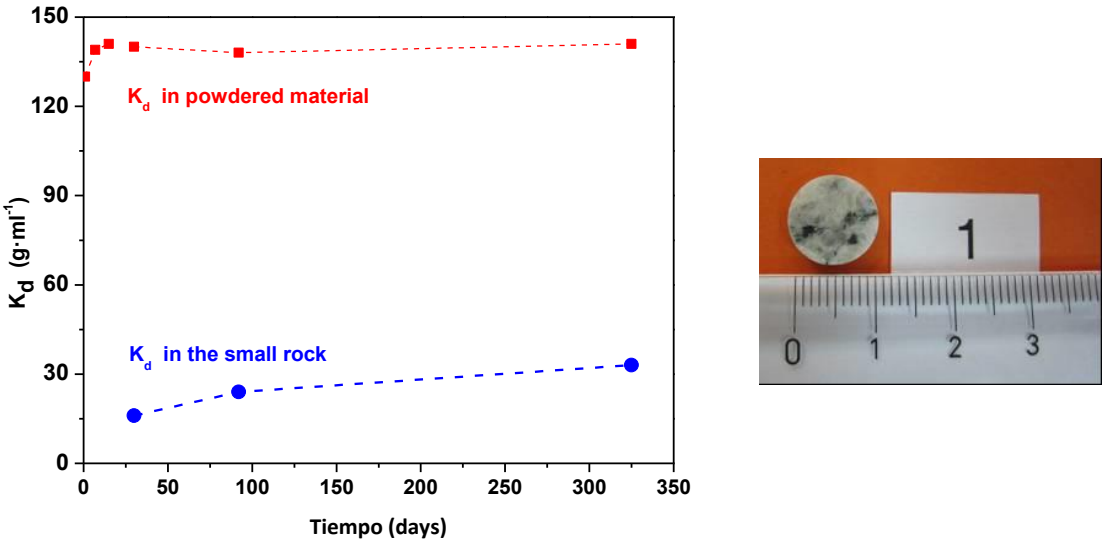

Figure 22.Comparison between the distribution coefficients of Cs ([Cs]=1·10^{-9} M) in granite obtained with powdered solid (red line) and in a small block of rock (blue points).

Diffusion experiments can be also useful to estimate K_d values on the intact rock by the determination of the effective diffusivity, D_e, and the rock capacity factor ($\alpha = \varepsilon + Kd\ \rho$), but it is not straightforward performing diffusion experiments in crystalline rocks and they are very time-consuming.

Undoubtedly, the use of different experimental techniques applied to the intact rocks is highly recommended to complement the knowledge gathered from detailed batch sorption experiments and very useful to promote the application of mechanistic models.

Different analytical techniques are available for the direct observation in coupons of the regions in which radionuclides adsorb (autoradiography methods, EDS, μPIXE, X-ray imaging mapping.) and the analysis of their mineralogy. This is useful to know what the most reactive minerals for a specific solute are. In granite, for example, Cs is almost always associated with biotite and its alteration products (e.g chlorite) and muscovite.

For example, Figure 23 shows by autoradiography (in red) the activity of ^{137}Cs in the granite surface, which is not homogeneous, compared to the regions in which mica minerals were identified (green). It is evident that Cs adsorbs preferentially on such minerals.

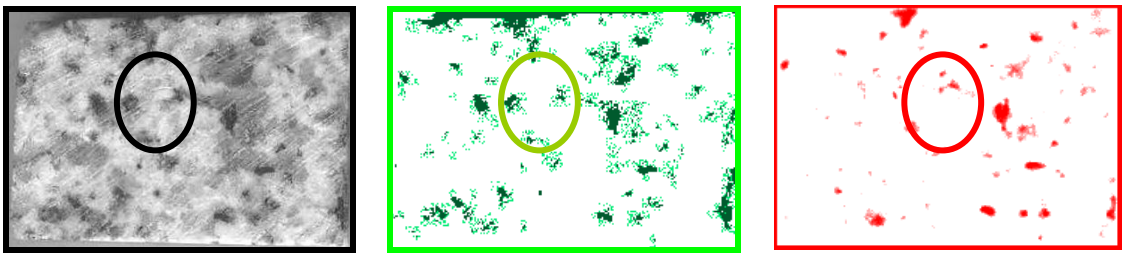

Granite | Micas distribution | ^{137}Cs activity after sorption

Figure 23.Image by autoradiography of ^{137}Cs sorption on a granite surface compared to the distribution of micas.

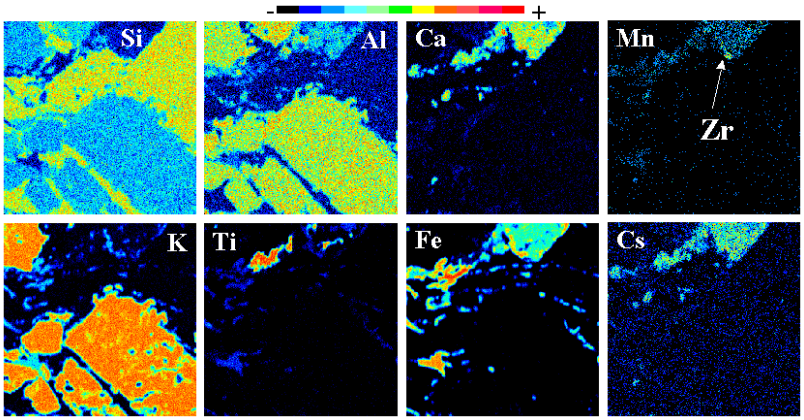

Figure 24. μPIXE images of granite rock surface where Cs was previously adsorbed.

Figure 24 shows a μPIXE image of a granite rock surface with the mapping of single elements in the solid in a 2x2 mm^2 area. In this surface, Cs was previously adsorbed. This technique allows identifying both the main minerals (through their elemental composition) and the reactive areas where the radionuclide is sorbed. It is evident, also in this case, that Cs sorption at the granite surface is not homogeneous.

The main challenge is still to quantify radionuclide retention at a mineral level, but nevertheless, these techniques help understanding how the distribution coefficients can be *up-scaled* in relation to the mineralogical heterogeneity and the "effective" reactive areas for each radionuclide.

It is of interest remarking that, in the same coupons, also other fundamental parameters can be determined, for example, porosity distribution and diffusion coefficients. The crossed information related to sorption and matrix diffusion helps achieving a more complete picture of retention. Sardini et al. (2007) proposed a model to simulate the heterogeneous diffusion in granite based on pore-scale images and assuming local values of diffusivities.

The further development of these o similar techniques is very promising for a better understanding of radionuclide retention in crystalline rocks (Missana *et al*., 2006).

7 CONCLUSIONS

The sorption of cesium on crystalline rocks of different origins has been analysed in the present study, considering the effects of pH, ionic strength, Cs concentration and the concentration of the main competitive ion potassium. Cesium adsorption is non-linear, in all analysed materials, indicating that more than one sorption site must exist on the surface of these rocks. This is somewhat expected considering the significant heterogeneity of the materials; furthermore, the dependence of sorption on pH (small) and ionic strength (significant) indicates that the main sorption mechanism is ionic exchange.

The study allowed identifying different factors that can affect the K_d determination and increase the uncertainty on the selection of this parameter amongst them, the most relevant: contact time, size fraction, Cs concentration and concentration of potassium in the aqueous solution.

Cesium sorption kinetics is almost negligible the finest rock samples used (<0.5 mm) but the time needed to reach sorption equilibrium increases as the size of the rock increases. The equilibration time could be considered an additional cause of error in K_d determination, if large fractions are used. The problem is not really related to the probably different surface area of the fractions, but to the fact that one must be sure that the sorption equilibrium has been reached. Furthermore, when the rock size fraction increases, the error attributable at the natural heterogeneity of the sample increases too.

Due to the non-linearity of Cs sorption, the radionuclide concentration represents one of the most important sources of variability on Cs distribution coefficients in these rocks. In the same rock, the K_d value can range within two or even three orders of magnitude. Thus, data from different source can be compared only if the radionuclide concentration is similar.

Part of the differences observed in the magnitude of distribution coefficients, from a material to another, can be explained by their BET surface area, as it can be assumed that a relation between the density of sorption sites and the BET area exist. Nevertheless, when the distribution coefficients are normalized to the BET area, other features appear providing interesting information. Considering the data from different rocks (at a selected Cs concentration) once normalised, the differences in the normalised K_d values, are not larger order of magnitude, and the mayor variations are observed at low Cs loadings. The effect of the presence of potassium in the aqueous phase is very important because it acts as a strong competing ion for sorption in the “strong” sites which dominate sorption at low Cs concentration. The presence of potassium must be always considered to understand the sorption behaviour of Cs.

At medium-high Cs concentrations, the BET-normalised K_d values obtained in the less saline water, were very similar for all the analysed rocks, being the swiss granite from the FEBEX tunnel at the GTS, *G-Feb* the only exception. The comparison of the shape of the sorption isotherm of this rock with that of the mineral potassium-feldspar, FdK, obtained under similar conditions, suggested that the different behaviour of the *G-FEB,* in respect to Cs adsorption, might be precisely related to its highest content of FdK.

A deeper knowledge of retention processes in such heterogeneous material requires the analysis of sorption processes in the principal minerals of the rock and further experiments are planned with single minerals, relevant for crystalline rocks as biotite, muscovite, K-feldspar or quartz. More detailed information is required to provide sound inputs for the mechanistic treatment of data and the application of thermodynamic models. Firs of all it is necessary a thorough revision of the experimental data verifying their coherence and comparability, as it is impossible apply a mechanistic model when uncertainties on the experimental data exist.

The modelling performed in this study, based on a top-down approach, aimed to correctly reproduce the main source of variability in the distribution coefficient of cesium (especially its concentration, ionic strenght and pH of the water, as well as the presence of main competing cations). The proposed model reproduced quite satisfactorily the data in all the analysed cases and represents a good starting point for the evaluation of Cs sorption data in a large number of crystalline rocks.

More information is needed for the extrapolation of K_d from batch experiment to field conditions and to asses the representativity of laboratory data or the methodology of their transferability to real systems (up-scaling). Sorption experiment on intact granite are expected to provide more realistic sorption values from beginning, and other additional information useful for the modeling of retention processes by mechanistic models.

8 REFERENCES

[1] Alonso U., Missana T., Patelli A., Ceccato D., García-Gutiérrez M., Rigato V. Se(IV) uptake by Äspö diorite: microscale distribution. Applied Geochemistry, 49, 87-94 (2014).

[2] André M., Malstrom M., Neretnieks I., Determination of sorption properties of intact rock samples: new methods based on electromigration. Journal of Contaminant Hydrology, 103, 71-81 (2009).

[3] André M., Neretnieks I., Malstrom M. Measuring sorption coefficients and BET surface area on intact drillcore and crushed granite samples. Radiochimica Acta, 96, 673-677 (2008)

[4] Bradbury M.H. & Baeyens B. A generalised sorption model for concentration dependent uptake of cesium by argillaceous rocks. Journal of Contaminant Hydrology, 42, 141-163 (2000).

[5] Chapman N.A. & Hooper A. The disposal of radioactive wastes underground, Proceedings of the Geologists' Association, 123, 46-63 (2012).

[6] Chapman N.A. & McKinley I.G. The geological disposal of nuclear waste, John Wiley & Sons (1987).

[7] Crafword J., Neretnieks I., Malstrom M. Data and uncertainty assessment for radionuclide portioning coefficients in granitic rock for use in SR-CAN calculations. SKB Technical Report TR-0675 (2006).

[8] Cui D. & Eriksen T. On the sorption of Co and Cs on Stripa granite fracture filling materials. Radiochimica Acta 79, 29-35 (1997)

[9] ENRESA, Almacenamiento geológico profundo de residuos radiactivos de alta actividad (AGP). Diseños conceptuales genéricos. Publicación Técnica 11/95. Madrid. 105 pp (2005).

[10] Fairhurst C. Nuclear waste disposal and rock mechanics: contributions of the Underground Research Laboratory (URL), Pinawa, Manitoba, International Journal of Rock Mechanics and Mining Sciences, 41, 1221-122 (2004).

[11] Gaines G.I. and Thomas H.C. (1953) "Adsorption studies on clay minerals II. A formulation of the thermodynamic of exchange adsorption" J. Chem Phys 21, 714-718.

[12] García-Gutierrez M. Experiencias preliminaries de migración de radionucleidos con materiales graníticos: El Berrocal (España). Publicación Técnica ENRESA 09/94 (1994)

[13] García-Gutierrez M., Yllera A., Mingarro M., Lopez V., Missana T. Cuantificación de parámetros de sorción y difusión en granitos y arcillas españoles. CIEMAT/DIAE/54231/8/99 (2000).

[14] Gómez P. Peña J., Buil B., Sánchez D.M., Sánchez L., Garralón B., de la Cruz B., Turrero M.J., Quejido A., Sánchez M., Bajos C. Características hidrogeoquímicas de las aguas subterráneas profundas del Macizo Hespérico (España). Journal of Iberian Geology, 32 (I), 113-132 (2006).

[15] Gómez P. Estudio del Impacto de la mina de uranio "Los Ratones" (Albalá, Caceres) sobre las aguas superficiales y subterráneas: modelación hidrogeoquímica. ENRESA Technical Report 06/2002 (2002)

[16] Hadermann J. & Heer W. The Grimsel (Switzerland) migration experiment: integrating firld experiments, laboratory investigation and modelling. Journal of Contaminant Hydrology, 21, 87-100 (1993).

[17] Hansen F. D., Hardin E. L., Orrell A. Geologic Disposal Options in the USA, International High-Level Radioactive Waste Conference 2011, Albuquerque, NM, American Nuclear Society. 13 934-940 (2011).

[18] Johnsson H., Siitari-Kauppi M., Skalberg M., Tullberg E.L. diffusion pathways in crystalline rock: examples from Aspo diorite and fined grained granite. Journal of Contaminant Hydrology 35, 41-53 (1998).

[19] Kienzler B, Bauer E., Schild D., Berotat W. Sorption of actinides on altered materials from Aspo HRL. Scientific basis for nuclear waste Management XXVII, 807, 665-670 (2004).

[20] Marcuello A., Gómez P., Carrera J., Ayora C. Muticomponent reactive transport modeling at the Ratones uranium mine, Cáceres (Spain) Journal of Iberian Geology 32(1) 133-146 (2006)

[21] McCombie C., McKinley I.G., Zuidema P. NAGRA performance assessment of radioactive waste disposal in crystalline and sedimentary host rocks, Proc. 1st Conf. High Level Waste Management (Las Vegas). 1 348-352 (1990).

[22] Miller W., Russel A., Chapman N., McKinley J.C., Smellie J. Geological Disposal of Radioactive Waste and Natural Analogues, Elsevier. (2000)

[23] Missana T. & García-Gutiérrez M., Analysis of sorption onto granite and granite minerals, the case of cesium. EC CP-Crock Final Workshop proceedings, 179-183, KIT-Scientific Publishing 7650 (2013).

[24] Missana T. & Geckeis H. Eds. The CRR Final Project Report Series II: Supporting laboratory experiments with radionuclides and bentonite colloids. NAGRA Technical Report NTB 03-02 (2006).

[25] Missana T., Alonso U., Patelli A., Rigato V., García-Gutierrez M. Retention processes in crystalline rocks: methodology for up-scaling Kd values accounting for sorption heterogeneity. First Annual Workshop proceedings of FUNMIG IP. CEA-R-6122 Rapport, 129-134 (2006)

[26] Missana T., Benedicto A., García-Gutiérrez M., Alonso U. Modelling of cesium retention onto Na-, K- and Ca-smectite: effects of ionic strenght, exchange and competing cations on the determination of selectivity coefficients. Geochimica et Cosmochimica Acta, 128, 266-277 (2014).

[27] Möri A., Alexander W.R., Geckeis H., Hauser W., Schafer T., Eickemberg J., Fiertz T., Degeldre C., Missana T. The colloid and radionuclide retardation experiment at the Grimsel Test Site: influence of bentonite colloids on radionuclide migration in a fractured rock. Colloid and Surface A 217, 33-47 (2003).

[28] Muuri E., Sittari-Kauppi M., Matara-aho M., Ikonen J., Lindberg A., Qian L., Koskinen L. Cesium sorption and diffusion on crystalline rocks: Olkiluoto case study. Journal of Radioanalytical Nuclear Chemistry, 311, 439-446 (2017).

[29] Payne T.E., Brendler V., Ochs M., Baeyens B., Brown P.L., Davis J.A., Eckberg C., Kulik D., Lutzenkirchen J., Missana T., Tachi Y., van Loon L., Altmann S. Guidelines for thermodynamic sorption modelling in the context of radioactive waste disposal Environmental Modelling and Software, 42,143-156 (2013)

[30] Poinssot C., Baeyens B., Bradbury M.H. Experimental and modelling studies of cesium sorption on illite. Geochimica et Cosmochimica Acta, 63, 3217-3227 (1999).

[31] Riekkola R., Saari J., Saksa P., Snellman M., Wikström L., Öhberg A., Final disposal of spent nuclear fuel in Finnish bedrock - Olkiluoto site report, POSIVA Report 99-10, Helsinki, pp.20 (1999)..

[32] Rivas P., Hernán P., Bruno J., Carrera J., Gómez P., Guimera J., Marin C., Perez del Villar L. El Berrocal Project Characterisation and validation of natural radionuclide migration processes under real conditions on the fissured granitic environment, Final Report EUR 17478 (1997)

[33] Samper J., Yang Q., Yi S., García-Gutierrez M., Missana T., Mingarro M. Interpretation of a laboratory mock-up experiment of the bentonite/granite interface with a numerical model, 4th Annual workshop Proceedings of the IP-FUNMIG, FZKA Publication 7461, 317-325 (2009).

[34] Sardini P., Robinet J.C., Siitari-Kauppi M., Dealy F., Hellmuth K.H. Direct simulation of heterogeneous diffusion and inversion procedure applied to an out-diffusion experiment. Test case of Palmottu granite. Journal of Contaminant Hydrology, 93, 21-37 (2007).

[35] Sawhney B.L. Potassium and cesium ion selectivity in relation to clay mineral. Clays and Clay minerals, 18, 47-49 (1970).

[36] Sawhney B.L. Selective sorption and fixation of cations by clay minerals: a review, Clays and Clay Minerals, 20, 93-100 (1972).

[37] Schneenberger R., Mader U., Weber H. Hydrochemical and isotopic characterization of fracturewater in crystalline rock (Grimsel, Switzerland) Procedia Earth and Planetary Science 17, 738-741 (2017).

[38] Stanfors R., Rhen I., Tullborg El., Wikberg P. Overview of geological and hydrogeological conditions of the Äspö Hard Rock Laboratory site. Applied Geochemistry 14(7), 819-834 (1999).

[39] Steinhouser G., Brandl A., Johnson T.E. Comparison of the Chernobyl and Fukushima nuclear accidents: a review of the environmental impacts. Science of the Total Environment, 470, 800-817 (2014).

[40] Sundberg J., Backb P.E., Christiansson R., Hökmark H., Ländell M., Wrafter J., Modelling of thermal rock mass properties at the potential sites of a Swedish nuclear waste repository. International Journal of Rock Mechanics and Mining Sciences. 46, 1042–1054 (2009).

[41] van der Lee J. and De Windt L., CHESS tutorial and cookbook, Technical Report LHM/RD/99/05 (1999)

[42] Yoshida H., Metacalfe R., Seida Y. Retardation capacity of altered granitic rock distributed along fractured and faulted zone in orogenic belt of Japan. Engineering Geology, 106, 116-122 (2009).

[43] Yoshida H., Takeuchi M., Metcalfe R., Long-term stability of flow-path structure in crystalline rocks distributed in an orogenic belt, Japan, Eng. Geol. (Amsterdam, Neth.), 78, 275–284. (2005)

[44] Zachara J.M., Smith S.C., Liu C.X., McKinley J.P., Serne R.J., Gassman P.L. Sorption of Cs+ to micaceous subsurface sediments from the Hanford site, USA. Geochimica et Cosmochimica Acta, 66, 193-211 (2002).

9 ANNEX

Mineral (%)	Central Aare granite	Grimsel Granodiorite	Grimsel Granodiorite	Mylonite
Quartz	33±3	28±3	32±3	30±3
Plagioglase/Albite	21±2	29±3	32±3	20±2
K-Feldspar	34±3	24±2	19±2	13±1
Biotite	7.3±1	11±1	9.1±1	21
Chlorite	7.3±1	11±1	1±0.1	0
Muscovite	1.7±0.2	3.4±0.3	2.3±0.2	21±2
Epidote	2.3	2	1.3	2.2
Sphene	Ac	Ac	Ac	Ac
Ilmenite	--	Ac	--	Ac
Allanite	Ac	Ac	Ac	Ac
Zircon	Ac	Ac	Ac	Ac
Apatite	Ac	Ac	Ac	Ac
Carbonate	<0.2	<0.2	<0.2	<0.1

Table A 1. Mineral contentin samples taken at GTS: Central Aare Granite, Grimsel Granodiorite, and Mylonite (fracture filling). Values extracted from the literature: Ac = Accesory.

MINERAL (%)	*Perdices*	*Cabeza Porquera*	*Megacristales*	*Millares*
Quartz	33-35	38-40	38-41	35-37
Plagioglase/Albite	29-32	23-26	18-20	25-27
K-Feldspar	26-28	28-30	33-35	26-28
Biotite/Chlorite	2-3	1-2	2-3	3-4
Muscovite	5-6	5-7	4-6	4-6
Accessory	Corderite Andalucite Ilmenite Anatase/Rutile Xenotime Monazite Zircon Uraninite	Turmaline Andalucite Zircon Rutile Apatite Monazite Xenotime	Cordierite Turmaline Zircon Apatite Monazite Xenotime	Andalucite Cordierite Turmaline Apatite Zircon Rutile Monazite Xenotime

Table A 2.Mineral content in samples from the Los Ratones mine.

BOREHOLE	SAMPLE REFERENCE	DEPTH (m)	TYPE
SR-1	SR1-CIE-MS-1	5.59-5.82	PERDICES
	SR1-CIE-MS-2	11.85-12.02	
	SR1-CIE-MS-3	50.15-50.25	
	SR1-CIE-MS-4	52.91-53.17	
	SR1-CIE-MS-5	65.28-65.71	
SR-2	SR2-CIE-MS-1	13.55-13.69	CABEZA PORQUERA
	SR2-CIE-MS-2	17.44	
	SR2-CIE-MS-3	24.41-24.52	
	SR2-CIE-MS-4	25.20-25.64	
	SR2-CIE-MS-5	44.84-45.09	
SR-3	SR3-CIE-MS-1	8.47-8.53	PERDICES
	SR3-CIE-MS-2	8.53-8.76	
	SR3-CIE-MS-3	42.59-42.89	
	SR3-CIE-MS-4	43.80-43.98	
	SR3-CIE-MS-5	80.57-80.87	
	SR3-CIE-MS-6	88.66-88.78	
	SR3-CIE-MS-7	89.45-89.64	
SR-4	SR4-CIE-MS-1	78.49-78.73	PERDICES
	SR4-CIE-MS-2	102.18-102.37	
	SR4-CIE-MS-3	107.35-107.58	
	SR4-CIE-MS-4	115.06-115.29	CABEZA PORQUERA
SR-5	SR5-CIE-MS-1	59.40-59.45	(FACIES COMUN)
	SR5-CIE-MS-2	140.70-140.81	MILLARES
	SR5-CIE-MS-3	255.17-255.33	PERDICES
	SR5-CIE- GR-1a(*)	321.57-322.56	
	SR5-CIE- GR-1b(*)	323.50-324.48	
	SR5-CIE-MS-4	421.63-421.87	
	SR5-CIE-MS-5	464.20-464.30	

* Reference

Table A 3 Samples used for sorption experiments from the "Los Ratones" mine

MINERAL (%)	FRESH (S-16 borehole)	WEATHERED (S-15 borehole)
Quartz	40-43	56.4
Plagioclase Albite	28-31	3.8
K-Feldspar	15-18	0.8
Biotite	1-2	--
Chlorite	1-2	--
Muscovite	7-9	39.3
Accessory	Zircon Anatase Monazite Xenotime Apatite Uraninite Thorite	

Table_A 4. Mineral content in samples from El-Berrocal. From Rivas et al (1997).

	FEBEX Tunnel (SJ5-3 borehole)	FEBEX Tunnel (FUN2-3 borehole)	MIGRATION Tunnel (AU96)
Na^+ (mg/L)	9.20 ± 0.01	11.00 ± 0.00	16.5
Ca^{2+} (mg/L)	7.80 ± 0.01	7.10 ± 0.00	6.6
Mg^{2+} (mg/L)	0.09 ± 0.01	0.08 ± 0.01	<0.4
K^+ (mg/L)	0.22 ± 0.01	0.17 ± 0.01	0.18
Sr^{2+} (mg/L)	nd	nd	0.21
Cl^- (mg/L)	0.28 ± 0.01	0.89 ± 0.03	7.7
SO_4^{2-} (mg/L)	7.90 ± 0.01	8.10 ± 1.13	6.1
F^- (mg/L)	3.80 ± 0.00	4.90 ± 0.00	6.4
Al (mg/L)	< 0.03	< 0.03	0.1
Fe (mg/L)	0.06	< 0.03	< 0.03
Cs (mg/L)	<0.02	<0.02	<0.02
Alk (meq/L)	0.57 ± 0.01	0.49 ± 0.01	
pH	8.69 ± 0.30	8.13 ± 0.60	9.5 ± 0.2
El. Cond. ($mScm^{-1}$)	60.00 ±1.00	65.00 ± 5.00	102 ± 5
SiO_2	0.08 ± 0.00	< 0.03	nd

Table A 5. Composition of different groundwaters sampled at the GTS (Switzerland).

	Los Ratones SR5 -T2 borehole	*El Berrocal* S2 borehole	Granitic Commercial Water
Na^+ (mg/L)	115	12	15
Ca^{2+} (mg/L)	7.2	35	47
Mg^{2+} (mg/L)	7.2	8.2	10
K^+ (mg/L)	2.8	0.76	1.1
Sr^{2+} (mg/L)	66	40	nd
Cl^- (mg/L)	26	5.2	12
SO_4^{2-} (mg/L)	8.9	3.9	14
F^- (mg/L)	0.37	1.7	0.18
Fe (mg/L)	0.13	3	nd
Mn (mg/L)	nd	0.59	nd
U(mg/L)	2	32	nd
HCO_3^- (mg/L)	321	166	148
pH	7.75	7.1	8.3
El. Cond. ($mScm^{-1}$)	578	272	282
SiO_2	23.1	33.7	20

Table A 6. Initial composition of waters from Los Ratones and El Berrocal (Spain). Data were taken from Gomez et al (2006)

	Äspö
Na^+ (mg/L)	1622-1894
Ca^{2+} (mg/L)	870-1135
Mg^{2+} (mg/L)	69.4-154
K^+ (mg/L)	10.5-48.6
Li+ (mg/L)	2.6-6
Sr^{2+} (mg/L)	13.8-19.9
Cl^- (mg/L)	4370-4999
SO_4^{2-} (mg/L)	296.2-394.4
F^- (mg/L)	1.35-1.51
Br- (mg/L)	19.1-23.2
Al (mg/L)	0.01-0.07
Fe (mg/L)	0.2-0.8
Mn (mg/L)	0.338-0.632
Alk (meq/L)	nd
pH	7.8-8
El. Cond. ($mScm^{-1}$)	11.75-13.31
Si	0.08 ± 0.00

Table_A 7. Composition of groundwater from Äspö Hard Rock Laboratory (Sweden)

FRACTION F1					FRACTION F2					FRACTION F3				
CONTACT TIME (days)	**15**	**60**	**120**	**LSW**	**CONTACT TIME (days)**	**15**	**60**	**120**	**LSW**	**CONTACT TIME (days)**	**15**	**60**	**120**	**LSW**
Na^+ (mg/L)	10.0±1.0	9.9±1.0	9.5±1.0	9.0±1.0	**Na^+ (mg/L)**	9.0±1.0	9.9±1.0	9.4±1.0	9.0±1.0	**Na^+ (mg/L)**	10.0±1.0	10±1.0	9.3±1.0	9.0±1.0
Ca^{2+} (mg/L)	13.0±1.0	16±1.0	16±1.0	7.6±0.1	**Ca^{2+} (mg/L)**	11±1.0	13±1.0	13±1.0	7.6±0.1	**Ca^{2+} (mg/L)**	9.8±0.1	12±1.0	13±1.0	7.6±0.1
Mg^{2+} (mg/L)	<0.03	0.14±0.02	0.13±0.02	<0.03	**Mg^{2+} (mg/L)**	0.04±0.02	0.06±0.02	0.06±0.02	<0.03	**Mg^{2+} (mg/L)**	0.04±0.02	0.06±0.02	0.05±0.02	<0.03
K^+ (mg/L)	7.6±0.2	3.3±0.2	3.3±0.2	<0.1	**K^+ (mg/L)**	Nd	5.5±0.2	6.0±0.2	<0.1	**K^+ (mg/L)**	12±0.2	5.7±0.2	3.5±0.2	<0.1
Cl^- (mg/L)	29±1	29±1	31±1	27±1	**Cl^- (mg/L)**	34.0±1.0	33±1.0	35±1.0	27±1	**Cl^- (mg/L)**	36±1	33±1	31±1	27±1
SO_4^{2-} (mg/L)	0.25±0.10	0.52±0.10	1.20±0.10	<0.1	**SO_4^{2-} (mg/L)**	0.13±0.10	0.25±0.10	1.4±0.10	<0.1	**SO_4^{2-} (mg/L)**	0.12±0.10	0.27±0.10	1.5±0.10	<0.1
F^- (mg/L)	1.1±0.2	2.3±0.2	2.3±0.2	<0.1	**F^- (mg/L)**	0.84±0.2	1.8±0.2	2.3±0.2	<0.1	**F^- (mg/L)**	0.7±0.2	1.2±0.2	2.3±0.2	<0.1
Al (mg/L)	0.2±0.05	0.13±0.05	0.17±0.05	<0.03	**Al (mg/L)**	0.05±0.02	0.04±0.02	0.05±0.02	<0.03	**Al (mg/L)**	<0.03	0.05±0.02	<0.03	<0.03
Fe (mg/L)	<0.03	<0.03	<0.03	<0.03	**Fe (mg/L)**	<0.03	<0.03	<0.03	<0.03	**Fe (mg/L)**	<0.03	<0.03	<0.03	<0.03
Mn (mg/L)	<0.03	0.07±0.05	0.09±0.05	<0.03	**Mn (mg/L)**	<0.03	<0.03	<0.03	<0.03	**Mn (mg/L)**	<0.03	<0.03	<0.03	<0.03
Cs (mg/L)	<0.02	<0.02	<0.02	<0.02	**Cs (mg/L)**	<0.02	<0.02	<0.02	<0.02	**Cs (mg/L)**	<0.02	<0.02	<0.02	<0.02
Eu (mg/L)	<0.03	<0.03	<0.5 (ug/L)	<0.03	**Eu (mg/L)**	<0.03	<0.03	<0.5 (ug/L)	<0.03	**Eu (mg/L)**	<0.03	<0.03		<0.03
U(mg/L)	0.89±0.04	2.3±0.04	1.4±0.04	0.26±0.04	**U(mg/L)**	0.96±0.04	0.92±0.04	1.6±0.04	0.26±0.04	**U(mg/L)**	1±0.04	1.8±0.04	1.9±0.04	0.26±0.04
Alk (meq/L)	0.32±0.02	0.46±0.02	0.40±0.02	<0.05	**Alk (meq/L)**	0.18±0.02	0.28±0.02	0.40±0.02	<0.05	**Alk (meq/L)**	0.15±0.02	0.23±0.02	0.24±0.02	<0.05
pH	7.63±0.2	Nd	7.41±0. 2	7.0±0.5	**pH**	7.60	Nd	7.47	7.0±0.5	**pH**	7.66	nd	7.54	7.0±0.5
Electrical conductivity	152.2±1.0	Nd	165.0±1.0	100±10	**Electrical conductivity**	157.8	Nd	157.4	100±10	**Electrical conductivity**	162.8	nd	147.7	100±10

Table A 8. Analysis of the variation of the chemistry of the LSW water with time after the contact with the different granite fractions. G-FEB granite

SAMPLE	S:L 50	S:L 20	S:L 12,5	S:L 10	FINAL pH	[Cs]	Mean Kd	Error (±)
SR1-CIE-MS-1	1,721	2,572	2,104	2,304	8.2-8.0	1.9E-8M	**2,175**	358
SR1-CIE-MS-2	838	916	913	682	8.1-7.9	1.9E-8M	**837**	109
SR1-CIE-MS-3	772	1,237	1,076	940	8.1-7.9	1.9E-8M	**1,006**	197
SR1-CIE-MS-4	1,620	3,089	2,955	3,000	8.1-7.9	1.9E-8M	**2,666**	699
SR1-CIE-MS-5	584	930	1,176	1,102	8.1-7.9	1.9E-8M	**948**	263
SR2-CIE-MS-1	1,565	1,827	1,842	1,849	8.1-8.1	2.1E-8M	**1,770**	137
SR2-CIE-MS-2	2,488	2,918	3,291	3,133	7.9-7.7	2.1E-8M	**2,957**	348
SR2-CIE-MS-3	1,010	1,209	1,367	1,482	8.1-7.8	2.1E-8M	**1,267**	204
SR2-CIE-MS-4	818	1,118	1,194	1,324	8.1-8.0	2.1E-8M	**1,113**	214
SR2-CIE-MS-5	384	521	593	641	8.2-8.0	2.1E-8M	**534**	111
SR3-CIE-MS-1	2,115	3,062	3,267	3,529	8.1-7.8	2.1E-8M	**2,993**	615
SR3-CIE-MS-2	1,431	1,923	2,176	2,336	8.2-8.0	2.1E-8M	**1,966**	395
SR3-CIE-MS-3	1,985	2,574	2,613	2,872	8.2-8.0	2.1E-8M	**2,511**	374
SR3-CIE-MS-4	1,634	1,718	2,150	1,823	7.9-7.6	2.4E-7M	**1,831**	226
SR3-CIE-MS-5	674	877	1,216	998	7.8-7.7	2.4E-7M	**941**	226
SR3-CIE-MS-6	575	815	1,010	855	7.9-7.8	2.4E-7M	**813**	180
SR3-CIE-MS-7	742	1,137	1,488	1,245	7.7-7.6	2.4E-7M	**1,153**	310
SR4-CIE-MS-1	1,036	1,266	1,342	1,446	8.2-7.8	2.1E-8M	**1,272**	174
SR4-CIE-MS-2	603	806	886	778	8.2-7.7	2.1E-8M	**768**	119
SR4-CIE-MS-3	555	637	674	716	8.2-7.9	2.1E-8M	**645**	68
SR4-CIE-MS-4	473	601	686	741	8.2-7.9	2.1E-8M	**625**	116
SR5-CIE-MS-1	759	782	792	904	7.9-7.7	2.1E-8M	**809**	64
SR5-CIE-MS-2	689	1,143	1,435	1,516	7.9-7.8	2.1E-8M	**1,195**	373
SR5-CIE-MS-3	474	800	1,019	995	8.0-7.8	2.1E-8M	**822**	251
SR5-CIE-MS-4	527	1,225	1,479	1,293	7.9-7.8	2.1E-8M	**1,131**	416
SR5-CIE-MS-5	455	1,716	1,990	2,062	8.0-7.8	2.1E-8M	**1,555**	748

Table A 9. K_d *values obtained in different samples of Rat granite. These tests were carried out with a commercial groundwater.*


9 788478 348251